Electronic Thesis and Dissertation Repository

9-9-2014 12:00 AM

Effects of Mixing and Vapor Residence Time on the Thermal Cracking Performance of Fluidized Beds

Clayton Stanlick, *The University of Western Ontario*

Supervisor: Cedric Briens, *The University of Western Ontario*
Joint Supervisor: Franco Berruti, *The University of Western Ontario*
A thesis submitted in partial fulfillment of the requirements for the Master of Engineering
Science degree in Chemical and Biochemical Engineering
© Clayton Stanlick 2014

Follow this and additional works at: https://ir.lib.uwo.ca/etd

Part of the Petroleum Engineering Commons

EFFECTS OF MIXING AND VAPOR RESIDENCE TIME ON THE THERMAL
CRACKING PERFORMANCE OF FLUIDIZED BEDS

(Thesis format: Integrated Article)

by

Clayton <u>Stanlick</u>

Graduate Program in Chemical and Biochemical Engineering

A thesis submitted in partial fulfillment
of the requirements for the degree of
Masters of Engineering Science

The School of Graduate and Postdoctoral Studies
The University of Western Ontario
London, Ontario, Canada

Abstract

The objective of this thesis is to investigate the effects of applied bed mixing and vapor phase residence time on the thermal cracking of agglomerating and non-agglomerating feedstock. Bitumen thermal cracking was investigated using a novel Mechanically Fluidized Reactor system and a pilot-scale Fluid Coking Reactor. Bed mixing and vapor residence time were studied to determine their impacts on agglomerate distributions, yields, and the quality of liquid product. Birchwood pyrolysis was investigated using a fluidized bed reactor to determine the impacts of particle bed mixing on the pyrolysis of a non-agglomerating feedstock, to provide contrast to the agglomerating bitumen-coke system.

It was observed that applied bed mixing destroyed agglomerates and dispersed the trapped reacting feedstock among smaller fragments, leading to reductions in coke yield and increased liquid production. Applied bed mixing resulted in lower viscosity, lower molecular weight liquid product at short vapor phase residence times. Prolonged vapor phase residence times facilitated the cracking of vapors into non-condensable gas, while increasing the concentration of more refractory, higher viscosity, higher molecular weight components in the liquid product. In addition, it was determined that the use of a feed system which disperses non-agglomerating biomass upon injection, in conjunction with a fluidized bed pyrolyzer, is an effective system and enhancing particle-feedstock mixing further provides no additional benefits for pyrolysis.

Keywords

Co-Authorship Statement

Chapter 2
Article Title:
Development of a Mechanically Fluidized Reactor System for Bitumen Thermal Crac
Authors:
Clayton Stanlick, Anil Jhawar, Cedric Briens, Franco Berruti
Article Status:
To Be Submitted
Experimental work, data analysis and writing were conducted by C. Stanlick. Revisio guidance and supervision were provided by A. Jhawar, C. Briens and F. Be

Chapter 3
Article Title:
Effects of Bed Mixing and Vapor Residence Time on Bitumen Thermal Cracking
Authors:
Clayton Stanlick, Cedric Briens, Franco Berruti
Article Status:
To Be Submitted
Experimental work, data analysis and writing were conducted by C. Stanlick. Revision, guidance and supervision were provided by C. Briens and F. Berruti.

Chapter 4
Article Title:
Effects of Bed Mixing on Biomass Fast Pyrolysis
Authors:
Clayton Stanlick, Cedric Briens, Franco Berruti
Article Status:
To Be Submitted
Experimental work, data analysis and writing were conducted by C. Stanlick. Revisio guidance and supervision were provided by C. Briens and F. Berruti.

Nothing in the world can take the place of persistence.

Talent will not; nothing is more common than unsuccessful men with talent.

Genius will not; unrewarded genius is almost a proverb.

Education will not; the world is full of educated derelicts.

Persistence and determination alone are omnipotent

Acknowledgments

Table of Contents

List of Tables

List of Figures

List of Appendices

Chapter 1

1   Introduction

In 2013, Alberta Energy Regulator estimated remaining *in situ* and mineable crude bitumen reserves of 167.2 billion barrels in Alberta. Initially established reserves in the region have only experienced 5.4 % of commercial production capacity within the past 50 years. Alberta remains Canada's largest contributor of oil production, with upgraded and non-upgraded bitumen consisting of 56% of Canada's oil and equivalent production in 2013. With Canada's proven oil reserves estimated to be the third largest in the world, coupled with unconventional oil resources considerably exceeding conventional oil, it is anticipated that bitumen upgrading will continue to represent a significant portion of worldwide petroleum production (Teare, Cruickshank, Miller, Overland, & Marsh, 2014) The depletion of worldwide conventional oil sources in recent years has led to a growing interest in unconventional resources including bitumen and biomass. The abundance and availability of these resources have fueled significant research and development into fuels from alternative resources.

Historically, conventional light crude oil reserves have been a major contributor to worldwide petroleum production. However, their ubiquitous use has lead to a shift towards unconventional oil resources such as bitumen and heavy and extra heavy crude oil (Shah et al., 2010). Alberta's oil sands contain a mixture of sand, clay, water and bitumen, approximately 18% of which can be processed through open-pit mining. The remaining 82% of proven bitumen reserves are recoverable through *in situ* processes such as cyclic steam stimulation, steam-assisted gravity drainage, and other emerging enhanced oil recovery technologies (Shah et al., 2010; Teare et al., 2014)

Bitumen is a complex mixture of high molecular weight aromatic hydrocarbons which exhibits a high viscosity and semi-solid state. It is characterized by relatively high levels of impurities such as nitrogen and sulphur heteroatoms, and metals such as nickel, copper, and vanadium (Hammond et al., 2003). After extraction, bitumen is typically fed through atmospheric and vacuum distillation to recover distillable fractions which can

then be upgraded separately through hydroprocessing. The distillable fractions of bitumen and heavy crudes are referred to as "bottom-of-the-barrel" residues that require significant processing in order to attain useful fuels. Delayed Coking and Fluid Coking€ are the most common unit operations applied to these residues (McCaffrey, Hammond, & Patel, 1998; Speight & Ozum, 2002). Delayed coking units and Fluid Coking reactors are capable of accepting a wide variety of feedstocks including atmospheric and vacuum topped bitumen which are far too heavy for other equipment to process effectively. The majority of impurities present in coker feeds are rejected into the solid coke product, nevertheless, impurity levels in coker naphtha and gas oils warrant further upgrading processes such as hydrotreating (Hammond et al., 2003; McCaffrey et al., 1998). The Syncrude operation involves hydrotreating and blending of coker naphtha and gas oils to produce a light, sweet synthetic crude that is transported to refineries in Canada and the United States for further refining into petroleum products.

1.1   Fluid Coking•

Fluid Coking€ is a non-catalytic carbon rejection process that is utilized to convert "bottom-of-the-barrel" residues into more valuable light and middle distillates. The process involves the main reactor, stripping and scrubbing sections, as well as a burner unit. The reactor section consists of a fluidized bed of hot coke particles into which bitumen is injected for thermal cracking into lower molecular weight compounds. The scrubbing section is situated on top of the reactor and cools the product vapors, effectively recycling heavier components back to the reactor while allowing lighter, more valuable products to exit (McCaffrey et al., 1998). The stripping section is employed to strip hydrocarbons from the surface of the bed coke in order to minimize hydrocarbons carry-under to the burner vessel. The burner vessel is a fluidized bed in which coke is partially combusted with oxygen to generate the heat requirements to sustain the endothermic cracking reactions. Hot coke is then recycled back to the reactor to complete the mass balance and continue the process while excess coke is quenched and stockpiled for future use (Hammond et al., 2003).

The reactor operates in the range of 510 to 565 °C, with maximum liquid yields occurring in the range of 515-530°C (Gray, 2002). Pressures are maintained close to atmospheric as

this favors vaporization of the product, however, in order to force the vapors through the scrubber and fractionator with greater ease, vapor pressures are typically around 2 atmospheres gauge (Gray, Le, & Wu, 2007; Pfeiffer, Borey, & Jahnig, 1959). The fluidized bed uses petroleum coke as a heat carrier as this provides very effective heat transfer to the incoming bitumen feed, allowing thermal cracking reactions to occur within the required timeframe (Gray, 2002). The average bed particle size is in the range of 75 to 500 micron, ideally in the range of 150 to 300 microns. Particles below 40 micron tend to agglomerate with each other, while larger particles result in defluidization issues. Stripping and atomization steam are injected at the rate of 6 to 15 wt% of the liquid feed to the reactor (Pfeiffer et al., 1959). Given the size of the equipment, this results in vapor phase residence times in the range of 15 to 30 seconds depending on where the vapors are liberated in the bed (Speight, 1998).

In terms of geometry, the stripping section is the smallest component of the Fluid Coker. The stripper is approximately 1.2 m in diameter, and occupies the lower 3 m of the reactor height. The stripper has the smallest cross section, as high superficial velocities are required to facilitate hydrocarbons stripping. Above the stripper, the main reactor section is comprised of an inverted cone and a cylindrical section with a maximum diameter of around 3.35 m. As the volumetric flowrate of vapors increases with height, the increasing cross section of the reactor zone allows for superficial velocity to held approximately constant across the entirety of the reactor. The main reactor section has a height of 15 m; giving a total fluidized bed height (including stripper) of 18 m. The reactor section then tapers off to form the disengagement zone. The disengager height is 6 m in order to accommodate cyclones and minimize solids entrainment into the scrubber. The reduced diameter of the disengager is designed to accelerate vapors and decrease the vapor phase residence time. The diameter further reduces in the scrubber which extends for up to 12 m to accommodate product fractionation. The burner vessel on the side of the reactor is of comparable diameter to the main reactor, with a height of around 10 m (Pfeiffer et al., 1959).

Bitumen is initially preheated in the range of 200 to 400 °C to reduce the viscosity and minimize the energy requirements of the reactor (Pfeiffer et al., 1959). Bitumen is mixed

with atomizing steam and injected into the fluidized bed via a series of atomization nozzles. In order to achieve uniform dispersion of liquid on the coke particles, 70 injection nozzles are located at varying heights and circumferential positions (Ariyapadi, 2004). The shear forces created at the nozzle tip break the bitumen into small droplets. Ideally, the droplets are dispersed evenly and coat individual coke particles in a thin film, however it is often observed that agglomeration occurs within the reactor through various means (Gray, 2002). Bitumen undergoes thermal cracking reactions due to heat transfer

Figure 1-1 - Fluid Coking Reactor[1]

from the coke particles. Bitumen thermally cracks into lower molecular weight compounds, which vaporize and leave behind a layer of fresh coke. The vapors travel up the reactor and into the disengagement zone where a series of cyclones remove any entrained coke particles and return them to the fluid bed via diplegs. The product vapors exit the cyclones and enter the scrubbing section.

Within the reactor vessel, there is a net upward flow of fluidization steam and product vapors. A counter-current flow of coke particles is maintained by constantly drawing off coke particles from the bottom of the bed, and recycling fresh coke to the top of the reactor. As the coke particles travel through the injection zone of the reactor, layers of fresh bitumen are laid down and product vapors are drawn off with each successive pass. The formation of fresh coke layers, coupled with agglomeration of wetted particles, causes the coke to grow in size (Gray, 2002). The larger particles have a higher propensity for falling to the bottom of the reactor, where they must be broken down using attrition nozzles. These attrition nozzles control the overall particle size distribution of the bed material by contacting the particles with high velocity steam. Gas velocities are in the range of 60-900 m/s to ensure effective agglomerate fragmentation (Pfeiffer et al., 1959). Solids travel through the attrition zone and then enter the stripping section of the reactor.

The scrubbing section located on top of the reactor is used to quickly cool the product vapors and condense any heavy fractions. Product vapors enter the scrubber at a temperature of 540 °C, and must be quenched below 400 °C to prevent cracking reactions (Jankovic, 1996). Cracking of products within the scrubbing section would result in coke formation and fouling of the internal structures, which decreases the efficiency of the scrubber and directly impacts the quality of the product oil. Fouling is a issue that also impacts the stripping section, however the environment in the scrubber can be more tightly controlled to alleviate this problem. As the vapors travel up the scrubber, they contact ,-shaped sheds. These sheds provide the contact between the hot vapor and colder liquid phases that is necessary to ensure effective heat transfer and condensation of heavy fractions (McKnight et al., 2011).

The cooling oil responsible for quenching the vapors is typically heavy gas oil recycled from the attached fractionation tower. Coker gas oil is the heaviest product fraction and is typically recycled to extinction, as this provides more valuable coker naphtha and middle distillates. The gas oil exiting the fractionator is cooled to 325 °C or lower and pumped into the scrubber to quench vapors. In addition, it is possible to inject feed directly into the scrubber to further assist in scrubing. The heavy compounds which are cooled and condensed by the heat exchange travel downwards by gravity, and enter the scrubber pool at the base of the scrubber. Here, the cooling oil (recycled heavy gas oil and any bitumen that has been injected) mixes with the cooled heavy fractions and is used to maintain the scrubber temperature below 400 °C. As the scrubber pool fills, this liquid is recycled back to the reactor for coking (Jankovic, 1996)

The solids recirculation pattern within the reactor vessel results in a downward flow of hot coke particles. As the particles travel from the reactor section to the stripper there are still small quantities of hydrocarbons on the surface of the particles, as well as in the interstitial space between downflowing solids. These hydrocarbons are a valuable product, and need to be removed from the coke to reduce carry-over to the burner vessel where they would otherwise be combusted. At the base of the stripper is a series of spargers which introduce fluidization steam to the reactor. Above the spargers are rows of stripper sheds which redistribute the fluidization gas along the entirety of the reactor cross-section. The sheds also have the effect of promoting effective contact between the fluidization gas bubbles and downflowing solid coke (Rose et al., 2005). As the gas bubbles and solid agglomerates meet, valuable hydrocarbons are stripped from the surface of the particles, travelling upwards through the reactor zone and into the scrubber (Davuluri, Bielenberg, Sutton, & Raich, 2011; Sanchez & Granovskiy, 2013)

At the bottom of the stripper section, coke particles are removed and pneumatically transported to the burner vessel using a dense-phase transfer line. The burner vessel operates in the range of 600-675°C and maintains a fuel-rich environment. Coke particles are discharged to the top of the burner, where they are partially combusted to generate the heat requirements for the reactor. Air is supplied to the bottom of the burner to fluidize the particles and supply elemental oxygen for combustion. Combustion rates in the

burner are in the range of 1-30% of coke produced in the reactor. Flue gas from the coke burner is typically fed to a carbon monoxide burner, pollution control equipment, and ultimately discharged to atmosphere. Net coke from the burner is cooled in a quench elutriator drum and sent to silos for storage. Hot coke is circulated back to the top of the reactor to complete the mass balance and supply the necessary heat for thermal cracking reactions to occur (Hammond et al., 2003; Speight, 1998)

Figure 1-2 - Typical Cracking Reactions (adapted from Gray et al. (2004))

With bitumen being a complex mixture of high-molecular weight hydrocarbons, resins, and asphaltenes, the chemical reactions are highly convoluted. A simplified model of the main chemical reactions is presented in Figure 1-2, through the use of lumped reactions. The heavy residues introduced into a Fluid Coker thermally crack into lower molecular weight gas oils and distillate material, which are fractionated and upgraded within a typical refinery. Heavy residue feeds also react to form a solid coke product as well as light and heavy residue fractions which can be recycled to extinction if necessary. The light residues within the liquid phase continue to react to vapor phase distillate and gas oils, and can also react to form coke precursors, leading to an increased coke yield under favorable conditions. The thermal cracking of a heavy residue feed yields distillate material (boiling under 343°C), light and heavy gas oils (343-524°C), light and heavy residues (524-650°C), and solid petroleum coke (Gray, McCaffrey, Huq, & Le, 2004)

1.2   Agglomeration in Fluidized Beds

Agglomerate formation in fluidized beds is a complex phenomenon impacted by various physicochemical properties of the bed material and liquid injection, as well as operating parameters of the equipment (Darabi, Pougatch, Salcudean, & Grecov, 2010). Poor liquid injection leads to loss of bed fluidity, entrapment of feed liquid in large agglomerates, reduced liquid yields, and severe fouling of reactor internals, all of which are detrimental to the performance of the Fluid Coking process (Gray, 2002; Sanchez & Granovskiy, 2013). Poor injection resulting in agglomeration requires bed reactor temperatures to be raised to reduce the likelihood of catastrophic defluidization, at the expense of valuable liquid yields (House, Saberian, Briens, Berruti, & Chan, 2004).

Ariyapadi et al. (2004) investigated the injection of gas-liquid jets into fluidized beds using non-intrusive digital x-ray imaging techniques. It was illustrated that agglomerate formation occurs at the end of the jet region. Agglomerates of 5 to 40 mm were observed in the low-shear regions of the jet, where the jet liquid contacts slow-moving particles (Ariyapadi, 2004). Weber et al. (2009) recently studied the effects of agglomerate properties on agglomerate stability in fluidized beds. Bitumen-coke agglomerates of varying sizes and liquid content were fluidized in a reactor at 530°C and fragmentation was observed. It was determined that high initial liquid-to-solid ratios in agglomerates led to a recruitment of bed coke particles and increased agglomerate size. However, the drying of liquid bridges within the agglomerates eventually led to an inability to recruit bed coke, and erosion began to fragment the larger agglomerate. Reduced liquid-to-solid ratios resulted in immediate erosion and fragmentation as the initial agglomerates did not have sufficient liquid to recruit more bed coke and maintain their size. In addition, larger agglomerates were found to fragment easier than their smaller counterparts, exposing a film of fresh liquid which was then able to bridge with bed material and reform small agglomerates (Weber, Briens, Berruti, Chan, & Gray, 2008; Weber, 2009). This is consistent with findings from Salman et al. (2003), who demonstrated a tendency of larger agglomerates to fragment at lower impact velocities (Salman, Fu, Gorham, & Hounslow, 2003).

Gray (2002) proposed a model of agglomerate formation through comparison with granulation in low-shear fluidized beds. In essence, the model suggests that the relatively large droplets introduced to the Fluid Coker impact bed solids during injection. Granulation processes dictate that the large droplets contact multiple smaller bed particles, forming an agglomerate with stable internal liquid bridges that would eventually dry to give a large agglomerate. However, the nature of the Coking process introduces shear forces which serve to break apart the initial agglomerate while it is still wet, dispersing the liquid film uniformly across the particles within the initial agglomerate. In addition, it is theorized that vapor production during the course of coking reactions destabilizes the initial wet agglomerates and allows for more even liquid dispersion (Gray, 2002).

It has been observed that coke product contains concentric layers of coke which have been deposited by successive passes through the feed section of the coker. Scanning electron images indicate coke layers in the range of 10 μm, suggesting that agglomerate breakage mostly disperses liquid films evenly across individual particles (Gray, 2002). Several authors have reported the impact of liquid film thickness on coking reactions using rapid induction heating of Athabasca vacuum residue (Gray et al., 2001, 2003, 2007; Gray et al., 2004). It was observed that the increase in film thickness led to a shift in transport phenomena of the product vapors. Thin films around 20 μm experienced passive diffusion of vapors, while films of ~80 μm predominantly experienced bubbling through thick films. In addition, thin films resulted in liquid yield increases on the order of 4 wt%, due to the reduction in mass transfer limitations imposed by thicker films (Gray et al., 2001, 2003, 2004).

Aminu et al. (2004) conducted experiments on the rapid heating of bitumen thin films in order to determine physical properties such as viscosity and surface tension at high temperature conditions. It was discovered that, for Athabasca vacuum residue at a reaction temperature of 530°C, the dry-out time for a 24-28 μm thin film is only 14.4 s. In addition, thin films still experienced large increases in viscosity as the reaction progressed, indicating that mass transfer limitations may still be present within the liquid films (Aminu, Elliott, McCaffrey, & Gray, 2004). However, a lack of viscosity data for

thicker films has yet to be remedied, and as a result it is difficult to characterize the reduction in mass transfer limitations by the use of thin films.

Ali et al. (2010) demonstrated the role of heat and mass transfer limitations in 2 mm agglomerates modeled after those produced in the Fluid Coking process. It was observed that agglomerate coke yields are insensitive to liquid saturation, temperature, and agglomerate thickness. This suggests that mass transfer plays a larger role than heat transfer within larger agglomerates, due to the longer diffusion path within agglomerates which have the capacity to increase the probability of coke-forming side reactions compared to thin films (Ali, Courtney, Boddez, & Gray, 2010). Gray (2001) indicates that retrograde reactions may exist as the fluid reacts. As coking reactions progress, the liquid transitions to a near-solid which has the capacity to trap volatiles, leading to additional coke-producing reactions (Aminu et al., 2004; Gray et al., 2001).

1.3 Pyrolysis

There is growing interest in obtaining fuels from alternative sources due to concerns over fossil-fuel depletion and the associated environmental impacts of fossil-fuel combustion. Renewable energy sources comprised 13% of global energy demand in 2010, with biofuels accounting for 3% of worldwide transportation fuels (International Energy Agency, 2012). Biomass pyrolysis is an attractive process which has the capability of converting agricultural and forestry wastes into liquid fuels. In addition to fuels, pyrolysis has the capability of producing high-value chemical products, thus lessening the dependence upon conventional fossil-fuels for their production (Mohan, Pittman, & Steele, 2006). This waste-to-fuels process has seen considerable research in previous decades due to its renewable feedstocks and the higher energy density of liquid product compared to raw biomass. As pyrolysis technology matures over the coming decades it may have the capacity to become a competitive source of fuels and energy in the global market.

Pyrolysis is the irreversible thermochemical degradation of material in the absence of oxygen. When applied to biomass, it is characterized by the fragmentation and conversion of high-molecular weight lignocellulosic compounds into low-molecular

weight liquid and gas products, with the deposition of char as a solid product. Pyrolysis can be applied to a variety of feedstocks for multiple applications. A significant portion of research has been conducted on wood due to its consistency as a feedstock, which allows for more accurate determination of reaction pathways and the impact of process parameters (Mohan et al., 2006). Nevertheless, pyrolysis has been carried out on biomass including potatoes, corn, sawdust, and sugarcane, as well varied compositions of their chemical constituents: cellulose, hemicellulose, and lignin (Drummond & Drummond, 1996; Isahak, Hisham, Yarmo, & Yun Hin, 2012; Nowakowski, Bridgwater, Elliott, Meier, & de Wild, 2010). In addition, research has been conducted on the pyrolysis of sewage sludge, waste wood and tires, and slaughterhouse waste for applications ranging from pollution control, landfill diversion, and renewable energy recovery (Dai et al., 2014; J. W. Kim et al., 2014; Martínez et al., 2013).

Biomass is a composite of cellulose, hemicellulose, and lignin, with small fractions of organic and inorganic compounds (Bridgwater, Meier, & Radlein, 1999). Cellulose is a very high molecular weight organic polymer comprising 40-50 wt% of most biomass, and begins to thermally degrade over the range of 325-400 °C. Hemicellulose is the second most abundant compound, and is a present anywhere from 25-35 wt% of most wood feedstock, and will degrade over the range of 200-300 °C. Lignin makes up a further 15-25 wt% of biomass and is an amorphous resin which takes on multiple structures. Lignin typically degrades over the range of 250-500 °C, although some researchers have observed reactions occurring between 100-900 °C (Mohan et al., 2006; Yang, Yan, Chen, Lee, & Zheng, 2007). The varying degradation temperature can be linked to the chemical changes that occur during lignin extraction from woody biomass, as well as the multiple structures that are characteristic of lignin. Biomass also contains small fractions of minerals and heavy metals that remain in the char product. Finally, depending upon the specific feedstock used, there are small fractions of organic extractives, such as proteins, simple sugars, and essential oils. As the solid biomass feedstock is rapidly heated, the macromolecular structure decomposes to evolve vapors and aerosols while leaving behind a solid-char product. The relative abundance of hemicellulose, cellulose, and lignin within the biomass feedstock directly influence the

chemical species found in the liquid product, as well as the total yields of solid, liquid and gas (Bridgwater et al., 1999; Mohan et al., 2006).

It has been shown that particle size plays an important role in the progress of particle drying, as well as primary and secondary pyrolysis reactions. As an individual particle is subjected to the high heat of the reactor, water trapped in the particle begins to vaporize and exit through the pores of the biomass particles. Primary reactions refer to the fragmentation and vaporization of the lignocellulosic compounds, resulting in permanent gases and condensable species. Primary reactions are responsible for the solid bio char that remains after pyrolysis. Secondary reactions refer to complex heterogeneous and homogeneous reactions that can occur between the char, permanent gases, and vaporized condensables, including reaction water. Secondary reactions encompass cracking, condensation, polymerization, gasification and oxidation reactions, among others, and can be both intraparticle and extraparticle (Ishak et al., 2012; Neves, Thunman, Matos, Tarelho, & Gómez-Barea, 2011).

With small particle sizes there is uniform heating, leading to rapid drying and primary reactions occurring within the particle. It is believed that the quick progression of drying and primary reactions facilitates quick vaporization and diffusion of the products, reducing the extent of intraparticle secondary reactions. Secondary reactions then occur in the vapor phase and can be controlled through the use of shortened residence times and quick quenching of condensable fractions. However, larger particles have been found to impose heat and mass transfer limitations, reducing the rate of drying and primary reactions. Due to the temperature gradient that develops from the outside of the particle to the inside, it is believed that drying and primary reaction fronts move sequentially, and can occur simultaneously at differing locations within the same particle. Consequently, as moisture and volatiles are exhausted from the outside layer of the particle, the resulting char layer acts as a barrier to the quick diffusion of water vapor and primary reaction products yet to be liberated from the inside of the particle. This would allow for an increased probability of secondary reactions occurring between the moisture, primary cracking products and char layer. In addition, pyrolysis progression increases the char

layer, adding a time dependency on the extent of intraparticle secondary reactions (Isahak et al., 2012; Neves et al., 2011)

It has been found that a reduction in particle size can improve liquid yields and lead to a reduction in char content, however the grinding process leads to cost increases that may not be offset by increased yields of valuable components (Isahak et al., 2012; S. Kim, Jung, & Kim, 2010). Ultimately, particle size has been demonstrated as having an impact on char, liquid, and gas yields, but is one of many parameters that must be taken into consideration for practical purposes. Optimization of particle size is of importance due to the grinding energy associated with smaller particles, but there is a trade-off between increased yields of valuable products and the energy input required to attain those yields (Isahak et al., 2012)

Although pyrolysis yields and product quality are directly influenced by the reactor configuration and operating parameters, there are specific ranges of heating rates, temperatures, and vapor residence time that lead to optimization of one product over another. The impact of temperature for pyrolysis has been well researched and documented. Pyrolysis is typically carried out in the range of 400-550 °C, while most woody biomass feedstocks have an optimum temperature in the range 450-550 °C (Mohan et al., 2006). The impact of temperature can be attributed to the relative concentrations of lignocellulosic material within the feedstock, as the degradation temperatures differ for each component (Bridgwater et al., 1999)

Slow pyrolysis is the mild form of pyrolysis operating with lower temperatures and longer residence times. This process utilizes large biomass particles in the range of 5 mm, with heating rates in the range of 0.1-1 °C/s. The larger particle size, coupled with the relatively low thermal conductivity of biomass, results in larger char formations under these conditions. In addition, slow pyrolysis utilizes vapor residence times of several minutes, promoting secondary reactions which convert liquid products to gas. Altogether, typical yields are in the range of 35 wt% char, 30 wt% liquid, and 35 wt% gas products (Bridgwater et al., 1999; Crocker, 2010). By modifying the process parameters to that of the fast pyrolysis regime it is possible to vastly increase the liquid yields.

Fast pyrolysis is characterized by high heating rates, controlled reaction temperature, and short vapor-phase residence times. Higher heating rates (≥1000 °C/s) coupled with more finely ground particles result in a reduction in char yield and greater evolution of product vapors. Furthermore, the reduced vapor residence times (<2 s) and quick quenching of product vapors allows for a reduction in secondary reactions in order to minimize the conversion of liquid products into gas. This combination of parameters allows for liquid yields on the order of 75-80 wt% of feed on a dry basis (Bridgwater et al., 1999).

The pyrolysis process can be carried out through a variety of reactor configurations. Bridgwater et al. (1999) provides a detailed overview of reactor types, of which there are three main classifications that are realizing commercial operation (Bridgwater et al., 1999). Fluid bed reactors are common due to the very effective heat transfer. The process requires the use of finely ground biomass to achieve the heating rates necessary to maximize liquid yields. However, the design allows for greater control over vapor residence time in order to minimize unwanted secondary cracking reactions. The downside with commercial units is the complexity of required char removal systems, as char catalyzes the secondary reactions into gas (Crocker, 2010). Ablative reactors employ pyrolysis by contacting large biomass particles with a heated surface at very high heating rates in order to "melt" the particles into an oil residue. The particles are then mechanically moved along the heat transfer surface, allowing a fresh particle surface to begin reacting. The oil residue then vaporizes and, after a short vapor residence time, exits the reactor for collection. Though this process allows for larger particles to be used, thus saving on the energy requirements of grinding, there are several drawbacks. The mechanical ablation within the reactor results in microcarbon which is entrained into the liquid product. The systems are also limited by the heat transfer capabilities of the heating surface (Bridgwater et al., 1999; Crocker, 2010). Finally, vacuum pyrolysis utilizes a slower heating rate and reduced temperatures. This requires a higher solids residence time but has the flexibility of accepting a larger particle size. As the vapors are evolved from the biomass, they are quickly drawn off under vacuum instead of carrier gas. This configuration experiences reduced liquid yields over fluid bed and ablative

pyrolyzers, in addition to a higher operational cost (Berruti, 2013; Bridgwater et al., 1999).

Pyrolysis yields are dependent upon feedstock, reactor configuration, and specific reactor parameters such as residence time and reaction temperature. Typical yields for fast pyrolysis of wood in a fluidized bed are 75 wt% liquid, with around 12 wt% char and 13 wt% gas on a dry wood basis (Crocker, 2010). The liquid product (bio-oil) is a dark brown liquid that often experiences phase separation during handling and transportation. It has a low pH in the range of 2-4. High oxygen concentrations in biomass result in oxygenated, reactive compounds in bio-oil. The high reactivity of these compounds leads to a complex series of condensation and polymerization reactions which ultimately results in instability and a short shelf-life (Mohan et al., 2006; Oasmaa & Peacocke, 2010). This yields an unstable product whose physical and chemical properties change irreversibly, particularly at elevated temperatures. Pyrolysis oil stabilization has been studied extensively to increase the shelf life of the oil, with some success found through catalyzed esterification of alcohols with the carboxylic acids present in the mixture (Zhang, Chang, Wang, & Xu, 2006).

Bio-oil is a complex mixture of chemical species which is difficult to characterize even with advanced analytical equipment. Generally, it is possible to perform solvent extractions and analyze separate fractions of the original product for analysis (Murwanashyaka, Pakdel, & Roy, 2001). Water content is typically on the order of 15-25 wt% (Bridgwater et al., 1999; Oasmaa & Peacocke, 2010). Polar organics such as acids, alcohols, ketones and aldehydes make up a further 30 wt% depending upon feedstock (Oasmaa & Peacocke, 2010). Sugars are also present in abundance due to the fragmentation of cellulose and hemicellulose, while the water-soluble fraction contains significant amounts of high molecular weight compounds linked to lignin decomposition (Mohan et al., 2006). Though there are several valuable chemicals whose pyrolysis pathways have been documented, levoglucosan (a sugar derived from cellulose degradation), acetic acid (derived from hemicellulose degradation) and phenolics (from lignin) are among the most abundant (Mohan et al., 2006; Murwanashyaka et al., 2001; Oasmaa & Peacocke, 2010).

The applicability of pyrolysis oil as a fuel is dependent upon the feedstock and chemical composition. Several successful attempts have been made with pyrolysis oil injection into gas turbines while achieving low pollutant emissions. Combustion in diesel engines has not seen any long-term success at this point, though efforts are still ongoing. As stabilization and upgrading techniques are improved upon, and grade specifications are developed, it is possible that bio-oil will become a competitive fuel in the future (Crocker, 2010; Oasmaa & Peacocke, 2010)

1.4 Research Objectives

The main objective of this thesis is to develop an understanding of the impacts of applied bed mixing and vapor phase residence time on the thermal cracking of agglomerating and non-agglomerating feedstock. For the agglomerating system, a new Mechanically Fluidized Reactor system is designed and implemented to investigate the impact of mechanical mixing on bitumen thermal cracking simultaneously for two vapor phase residence times. Bed mixing and vapor phase cracking can thus be studied to determine their impacts on the yield and quality of the liquid product. A Fluid Coking Reactor is then investigated to quantify the impacts of applied bed mixing and vapor residence time within a more traditional fluidized system. Finally, birchwood pyrolysis is conducted in a fluidized bed to compare the impacts of applied bed mixing in agglomerating and non agglomerating systems.

1.5 References

Ali, M., Courtney, M., Boddez, L., & Gray, M. (2010). Coke Yield and Heat Transfer in Reaction of Liquid–Solid Agglomerates of Athabasca Vacuum Residue. The Canadian Journal of Chemical Engineering, 88(1), 548.

Aminu, M. O., Elliott, J. A. W., McCaffrey, W. C., & Gray, M. R. (2004). Fluid Properties at Coking Process Conditions. Industrial & Engineering Chemistry Research, 43(12), 2929–2935.

Ariyapad, S. (2004). Interaction Between Horizontal Liquid Jets and Gas–Solid Fluidized Beds. The University of Western Ontario.

Berruti, F. M. (2013). Development and Applications of a Novel Intermittent Solids Feeder for Pyrolysis Reactors. The University of Western Ontario.

Bridgwater, A. V, Meier, D., & Radlein, D. (1999). An Overview of Fast Pyrolysis of Biomass. Organic Geochemistry, 30, 1479–1493.

Crocker, M. (Ed.). (2010). Thermochemical Conversion of Biomass to Liquid Fuels and Chemicals. Cambridge: Royal Society of Chemistry.

Dai, Q., Jiang, X., Jiang, Y., Jin, Y., Wang, F., Chi, Y., & Yan, J. (2014). Formation of PAHs During the Pyrolysis of Dry Sewage Sludge. Fuel, 130, 92–99.

Darabi, P., Pougatch, K., Salcudean, M., & Grecov, D. (2010). Agglomeration of Bitumen-Coated Coke Particles in Fluid Cokers. International Journal of Chemical Reactor Engineering, 8.

Davuluri, R. P., Bielenberg, J. R., Sutton, C. R., & Raich, B. A. (2011). Fluid Coking Unit Stripper. United States: United States Patent Office.

Drummond, A. R. F., & Drummond, I. W. (1996). Pyrolysis of Sugar Cane Bagasse in a Wire-Mesh Reactor. Industrial & Engineering Chemistry Research, 35(4), 1263–1268.

Gray, M. R. (2002). Fundamentals of Bitumen Coking Processes Analogous to Granulations : A Critical Review. The Canadian Journal of Chemical Engineering, 80(June), 393–401.

Gray, M. R., Le, T., McCaffrey, W. C., Berruti, F., Soundararajan, S., Chan, E., & Thorne, C. (2001). Coupling of Mass Transfer and Reaction in Coking of Thin Films of an Athabasca Vacuum Residue. Industrial & Engineering Chemistry Research, 40, 3317–3324.

Gray, M. R., Le, T., & Wu, X. A. (2007). Role of Pressure in Coking of Thin Films of Bitumen. The Canadian Journal of Chemical Engineering, 85(October), 773.

Gray, M. R, McCaffrey, W. C., Huq, I., & Le, T. (2004). Kinetics of Cracking and Devolatilization during Coking of Athabasca Residues. Industrial & Engineering Chemistry Research, 43(18), 5438–5445.

Gray, M. R., Zhang, Z., McCaffrey, W. C., Huq, I., Boddez, L., Xu, Z., & Elliott, J. a. W. (2003). Measurement of Adhesive Forces during Coking of Athabasca Vacuum Residue. Industrial & Engineering Chemistry Research, 42(15), 3549–3554.

Hammond, D. G., Lampert, L. F., Mart, C. J., Massenzio, S. F., Phillips, G. E., Sella, D. L., & Woerner, A. C. (2003). Review of Fluid Bed Coking Technologies (pp. 1–8).

House, P. K., Saberian, M., Briens, C. L., Berruti, F., & Chan, E. (2004). Injection of a Liquid Spray into a Fluidized Bed: Particle–Liquid Mixing and Impact on Fluid Coker Yields. Industrial & Engineering Chemistry Research, 43, 5663–5669.

International Energy Agency. (2012). World Energy Outlook 2012. Paris.

Isahak, W. N. R. W., Hisham, M. W. M., Yarmo, M. A., & Yun Hin, T. (2012). A Review on Bio-oil Production from Biomass by Using Pyrolysis Method. Renewable and Sustainable Energy Reviews, 16(8), 5910–5923.

Jankovic, J. (1996). Simulation of the Scrubber Section of a Fluid Coker. University of Belgrade.

Kim, J. W., Lee, H. W., Lee, I.-G., Jeon, J.-K., Ryu, C., Park, S. H., & Park, Y.-K. (2014). Influence of Reaction Conditions on Bio-oil Production from Pyrolysis of Construction Waste Wood. Renewable Energy, 65, 41–48.

Kim, S.-J., Jung, S.-H., & Kim, J.-S. (2010). Fast Pyrolysis of Palm Kernel Shells: Influence of Operation Parameters on the Bio-oil Yield and the Yield of Phenol and Phenolic Compounds. Bioresource Technology, 101(23), 9294–9300.

Martínez, J. D., Puy, N., Murillo, R., García, T., Navarro, M. V., & Mastral, A. M. (2013). Waste Tyre Pyrolysis – A Review. Renewable and Sustainable Energy Reviews, 23, 179–213.

McCaffrey, D. S., Hammond, D. G., & Patel, V. R. (1998). Fluidised Bed Coking Utilising Bottom of the Barrel (pp. 1–7).

McKnight, C. A., Hackman, L. P., Knapper, B. A., Bulbac, D., Jones, G. B., Tyler, J., & Kiel, D. E. (2011). Scrubber for Fluid Coker Unit. United States: United States Patent Office.

Mohan, D., Pittman, C. U., & Steele, P. H. (2006). Pyrolysis of Wood/Biomass for Bio-oil: A Critical Review. Energy & Fuels, 20(3), 848–889.

Murwanashyaka, J. N., Pakdel, H., & Roy, C. (2001). Separation of Syringol from Birch Wood-Derived Vacuum Pyrolysis Oil. Separation and Purification Technology, 24, 155-165.

Neves, D., Thunman, H., Matos, A., Tarelho, L., & Gómez-Barea, A. (2011). Characterization and Prediction of Biomass Pyrolysis Products. Progress in Energy and Combustion Science, 37(5), 611-630.

Nowakowski, D. J., Bridgwater, A. V., Elliott, D. C., Meier, D., & de Wild, P. (2010). Lignin Fast Pyrolysis: Results from an International Collaboration. Journal of Analytical and Applied Pyrolysis, 88(1), 53-72.

Oasmaa, A., & Peacocke, C. (2010). Properties and Fuel Use of Biomass-Derived Fast Pyrolysis Liquids.

Pfeiffer, R. W., Borey, D. S., & Jahnig, C. E. (1959). Fluid Coking of Heavy Hydrocarbons. United States: United States Patent Office.

Rose, I., Cui, H., Zhang, T., McKnight, C., Grace, J., Bi, X., & Lim, J. (2005). Towards an Ultimate Fluidized Bed Stripper. Powder Technology, 158(1), 124-132.

Salman, A. D., Fu, J., Gorham, D. ., & Hounslow, M. (2003). Impact Breakage of Fertiliser Granules. Powder Technology, 130(1), 359-366.

Sanchez, F. J., & Granovskiy, M. (2013). Application of radioactive particle tracking to indicate shed fouling in the stripper section of a fluid coker. The Canadian Journal of Chemical Engineering, 91(6), 1175-1182.

Shah, A., Fishwick, R., Wood, J., Leeke, G., Rigby, S., & Greaves, M. (2010). A Review of Novel Techniques for Heavy Oil and Bitumen Extraction and Upgrading. Energy & Environmental Science, 3(6), 700.

Speight, J. G. (1998). Petroleum Chemistry and Refining. Washington: Taylor & Francis.

Speight, J. G., & Ozum, B. (2002). Petroleum Refining Processes. New York: Marcel Dekker.

Teare, M., Cruickshank, R., Miller, S., Overland, S., & Marsh, R. (2014). Alberta's Energy Reserves 2013 and Supply/Demand Outlook 2014-2023. Calgary.

Weber, S., Briens, C., Berruti, F., Chan, E., & Gray, M. (2008). Effect of Agglomerate Properties on Agglomerate Stability in Fluidized Beds. Chemical Engineering Science, 63(17), 4245-4256.

Weber, S. (2009). Agglomerate Stability in Fluidized Beds. The University of Western Ontario.

Yang, H., Yan, R., Chen, H., Lee, D. H., & Zheng, C. (2007). Characteristics of Hemicellulose, Cellulose and Lignin Pyrolysis. Fuel, 86(12), 1781-1788.

Zhang, Q., Chang, J., Wang, T., & Xu, Y. (2006). Upgrading Bio-Over Different Solid Catalysts. Energy & Fuels, 20(6), 2717-2720.

Chapter 2

2 Development of a Mechanically Fluidized Reactor System for Bitumen Thermal Cracking

2.1 Introduction

Bitumen upgrading involves several unit operations, with Delayed Coking and Fluid Coking€ being the most common. Fluid Coking€ is a noncatalytic process that is utilized to thermally crack heavy residues into light and middle distillates that can then be upgraded into transportation fuels and petrochemicals (McCaffrey, Hammond, & Patel, 1998; Speight & Ozum, 2002). Inside the Fluid Coker, bitumen is injected through a series of atomization nozzles. The fine bitumen droplets contact a hot bed of petroleum coke, thermally cracking into lighter products while leaving behind a layer of fresh petroleum coke. As the bitumen interacts with coke particle, the formation of liquid-solid agglomerates is typically experienced. Agglomeration is detrimental to the performance of fluidized beds, resulting in entrapment of feed liquid and severe fouling of reactor internals. The consequences are reduced yield of valuable liquids and increased solid coke formation (Gray, 2002; House, Saberian, Briens, Berruti, & Chan, 2004; Sanchez & Granovskiy, 2013). Detailed description of the Fluid Coking process and operating parameters can be found in Chapter 1.

Several authors have reported the impact of agglomerate properties (Ariel. et al., 2010; Salman et al., 2003; Weber et al., 2008; Weber, 2009) as well as bitumen film thickness (Aminu et al., 2004; Gray et al., 2001, 2003, 2007) on cracking reactions. Together, the results using both large agglomerates and thin films indicate that quick breakage of agglomerates assists in the dispersion of liquid uniformly across the bed particles. A transition from large agglomerates to a thin film on the surface of a small agglomerate would allow for a reduction in mass and heat transfer limitations, theoretically leading to faster cracking reaction rates. A more in-depth discussion of the impacts of agglomerate properties and bitumen film thickness can be found in Chapter 1.

Chaudhari (2012) investigated the impact of bed material and mixing on oil-solid contact for heavy oil thermal cracking. A Mechanically Fluidized Reactor was utilized to study vapor evolution from the reactor while reactor operating parameters were varied. Increased bed mixing was found to increase liquid and gas yields for heavy oil. It was also found that increased bed mixing led to a reduction in the time required to vaporize liquid trapped within the bed (Chaudhari, 2012). This study suggests that improved liquid yields can be attained, though agglomeration and liquid quality were not investigated, nor was the impact of vapor residence time on liquid and gas yields.

The main objective of this study is to develop a Mechanically Fluidized Reactor system to investigate the impacts of bed mixing on aggregate distributions produced during bitumen thermal cracking. The reactor is designed to decouple the reactor bed from the freeboard, in order to investigate the impact of two separate vapor phase residence times simultaneously while reducing intrinsic experimental errors that may arise from the reactor bed during normal operation.

Quantification of the impact of applied bed agitation on agglomerate distributions and corresponding impact on Fluid Coking yields is accomplished using continuous bitumen injection into the Mechanically Fluidized Reactor. Separate vapor phase residence times are employed to estimate the impact of vapor phase cracking on liquid and gas yields. Bed mixing and vapor phase cracking are also investigated to quantify their impact on product oil quality. Finally, experiments determine the maximum liquid yield attainable from the reactor system, and the corresponding level of applied mechanical agitation.

2.2 Experimental

2.2.1 Materials

The feed to the reactor was Athabasca vacuum topped bitumen provided by Syncrude Canada Ltd. This feed represents the non-distillable residue from vacuum distillation. The bitumen specific gravity was approximately 1.01, and viscosity values at various temperatures are provided in Figure 2-1. Molecular weight analysis indicated that the feed had a weight-averaged molecular weight of 1945 g/mol, with a polydispersity of 4.2.

Ultimate elemental analysis indicated that the bitumen had a carbon-hydrogen ratio of 8.4, and elemental composition is reported in Table 2-1.

Table 2-1 - Bitumen specifications

Ultimate Elemental Analysis:		
Carbon	82.1	wt%
Hydrogen	9.8	wt%
Nitrogen	0.6	wt%
Sulphur	5.3	wt%
Oxygen (by difference)	2.2	wt%
Weight-Averaged Molecular Weight	1945	g/mol
Specific Gravity	1.01	

Nitrogen was used as fluidization, atomization, and makeup gas as it allows for an oxygen-free environment suitable for thermal cracking reactions. The reactor bed was composed of petroleum coke having a particle density of 1450 kg/m^3 and a Sauter mean diameter of 140 …m. Total bed mass was held constant at 0.400 kg for each experiment. In order to maintain consistent bed conditions over the course of experimentation, bed coke samples were analyzed in a Sympatec Helos/BF Particle Size Analyzer prior to experimentation.
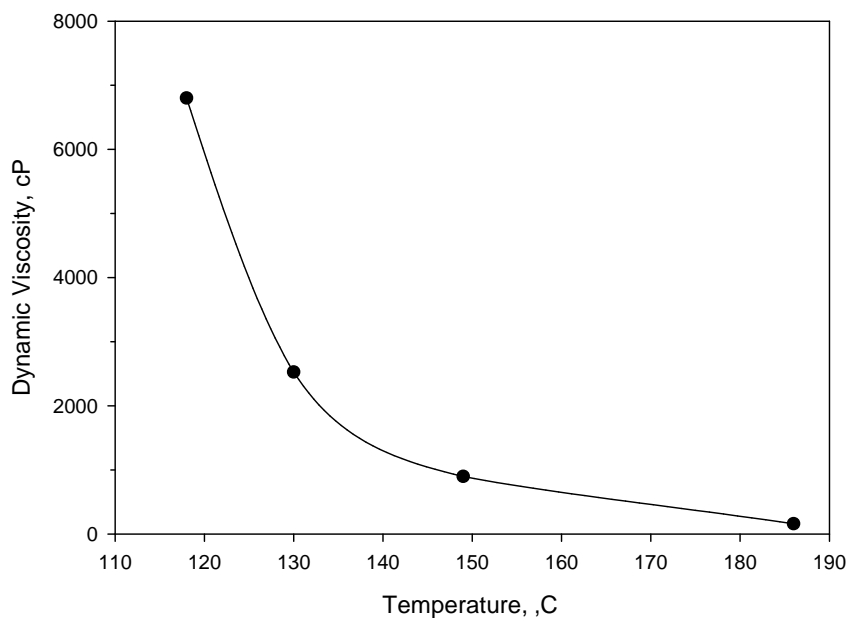
Figure 2-1 - Bitumen viscosity

2.2.2   Experimental Apparatus

Experiments were conducted a novel Mechanically Fluidized Reactor (MFR) system. The MFR had a 0.091 m internal diameter and a height of 0.127 m. The coke bed height in the reactor was maintained at 0.07 m for each experiment. The reactor was operated at 530 °C and atmospheric pressure.

Figure 2-2 - MFR schematic

The mixing system was mounted on the top of the reactor, with the driveshaft located in the center of the reactor flange. The mixer blade was driven by an electric variable speed motor, allowing for mechanical agitation speeds ranging from 20 to 200 RPM. The mixer

blade orientation in the reactor was such that it scraped the wall of the reactor and drew solids into the center of the bed. Nitrogen gas and bitumen feed were injected into the top of the reactor using a double pipe injection system, as shown in Figure 2-2.

A secondary tube reactor was fitted downstream of the MFR to provide prolonged vapor phase cracking of a portion of the product to simulate the freeboard cracking in the fluid coker (Figure 2-3). This cylindrical reactor had an internal diameter of 0.063 m, with a total internal length of 0.310 m. The vapor exit was fitted with a filter to prevent solids entrained with the product vapor from entering the liquid collection systems.

Figure 2-3 - Tube reactor schematic

The Mechanically Fluidized Reactor and tube reactor were designed and built with a custom induction heating system (Appendix E). Each system contained an 1800 W induction heater (Hannex, Hong Kong, China). Temperature readings for the reactor system were acquired using four type K thermocouples, one 9211 thermocouple input (National Instruments, Austin, TX), and one 9485 8-channel solid state relay (National Instruments, Austin, TX). A program created in the LabWindows€/CVI platform (National Instruments, Austin, TX) collected the temperature signals and used on-off control to power the induction heaters. Temperature control was provided for the MFR and tube reactor, while temperature monitoring was provided for the bitumen injection pump and the product line between the MFR and tube reactor.

2.2.3   Experimental Procedure

Bitumen was fed to the reactor through the use of a dual piston pump. Bitumen was preheated to a temperature of approximately 125 °C in the top chamber of the pump. Hydraulic oil was pumped into the bottom chamber at a constant flowrate, forcing the piston upwards. This pressurized the bitumen chamber and displaced the oil into the injection line at a constant flowrate. The injection line was maintained at a temperature of approximately 200 °C.

Bitumen was injected from the top of the reactor through the inner tube of a double pipe feeding system. Nitrogen gas was injected through the outer tube, and was used to assist in controlling the vapor phase residence time. The bitumen thermally cracked to lower molecular weight products, which vaporized and deposited a layer of fresh coke on the original bed coke particles. The product gases and vapors exited the reactor through the mixer driveshaft, as seen in Figure 2-2. The product stream between the MFR and tube reactor was left unheated, allowing the product vapors to cool to a temperature in the range of 180 to 200 °C through heat exchange with ambient air. This temperature has been found sufficient to reduce secondary reactions, while reducing backpressure issues caused by vapor product condensation. The product line was then split into two separate streams in order to study the impact of vapor phase residence time. Approximately 60% of the products were immediately quenched using a condenser immersed in an ice bath. The remaining 40% of the products were diverted to the tube reactor, where they were heated back to 530 °C to undergo further thermal cracking reactions. Immediately after the tube reactor was a condenser to quench the liquid product.

Both product streams were equipped with a single condenser immersed in an ice bath, followed by a high-efficiency electrostatic precipitator (ESP). Heavy fractions of the oil were collected in the bottom of the condensers, while non-condensable gases and entrained mist continued downstream. Within the ESP, a voltage of 15 kV was applied between the electrode and ESP wall, resulting in ionization of the gas around the electrode through corona discharge. The entrained mist entering the ESP was charged by the ionized gas, and the electric field around the electrode forced the charged mist to the wall. Mist condensed on the wall and drained to the bottom of the ESP for collection.

Figure 2-4 - MFR process diagram

non-condensable gases continue through a cotton filter and were sampled for subsequent gas analysis. Exhaust gas from both product streams was combined and vented to atmosphere.

Control over the split ratio of the product streams and determination of the reactor yields was accomplished through rotameter control prior to gas sampling (Figure 2-4). During experimentation, the vapor exit stream was split to a determined ratio of flowrates in order to achieve the desired residence times in each product stream. Analysis of the product gas from each stream then provided gas composition data, which was used to determine the rotameter correction factors and provide the true flowrates of vapors travelling through the rotameters. True vapor flowrates were then used to determine the true split ratio, providing yields and residence times for each product stream.

The mass change of the condensers, electrostatic precipitator, and filter were used to determine the liquid yield. Gas composition data and gas flowrates were used to determine the gas yield. Coke yield was first estimated from the mass change of the reactor bed. Due to slight variability in bed material volatiles content, the coke yields are reported by difference to provide more accurate determination of the impacts of mechanical agitation.

Table 2-2 - MFR operating conditions

Shorter Vapor Phase Residence Time	s	4.9
Longer Vapor Phase Residence Time	s	10.6 ± 0.21
Injection Rate	mL/min	5.6
Injection Time	min	40
MFR Temperature	°C	530 ± 3
Tube Reactor Temperature	°C	530 ± 5
MFR Pressure	psig	0

The impacts of applied bed mixing and vapor phase residence time were studied at a single reactor temperature of 530°C. Bitumen was preheated to a temperature of approximately 120-125 °C in a double piston pump and injected at a rate of 5.6 mL/min. Injection was continuous over the course of 40 minutes in order to obtain the sample volumes required for analysis and reduce errors in measurement.

Experimentation was initially performed using a bed drying period of 45 s after injection was stopped. It was then determined that a 45 s drying period was not sufficient to completely dry out the bed under poorly mixed conditions as there were still minute quantities of unvaporized liquid trapped in the larger agglomerates. A drying time of 20 minutes was then used to determine the true liquid and coke yields under the poorly mixed condition. As such, the reported values for poorly mixed conditions represent the true liquid and coke yields with 20 minutes of bed drying.

Statistical analysis using replicate experiments has been performed to determine the impact of mixing and vapor phase cracking. Significance has been tested using a one tailed comparison of means in most cases, with two tailed comparisons being used where appropriate. Statistical significance is reported through the use of p values; these values represent the probability that any differences between the data sets can be attributed to random error.

2.2.4   Analysis

In order to determine the extent of cracking reactions, density and viscosity of the product oil were analyzed using an Anton Paar SVM 3000 Viscometer at a temperature of 60 °C. In addition, the relative molecular weight of the product liquid were measured with a Waters Breeze GPC-HPLC (Gel Permeation Chromatography-High Performance Liquid Chromatography) instrument (1525 binary pump, Waters Styrylgel HR1 column at a temperature of 40 °C; UV detector at 270 nm). The GPC-HPLC was calibrated with linear polystyrene standards, and utilized THF as an eluent at a flow rate of 1 ml/min. The composition of gaseous components was found using two Varian 490 CP3 Column Micro Gas Chromatographs.

2.3 Results and Discussion

2.3.1   Agglomerate Distributions

Within the MFR, it was observed that agglomerates were present ranging from 355 µm to over 9500 µm. Small agglomerates were present in abundance, while large agglomerates were far less common. However, larger agglomerates introduce heat and mass transfer limitations within the reactor, which result in slower reaction rates, longer diffusion pathways for product vapors, and a higher probability of coking side reactions (Gray et al., 2001, 2004).
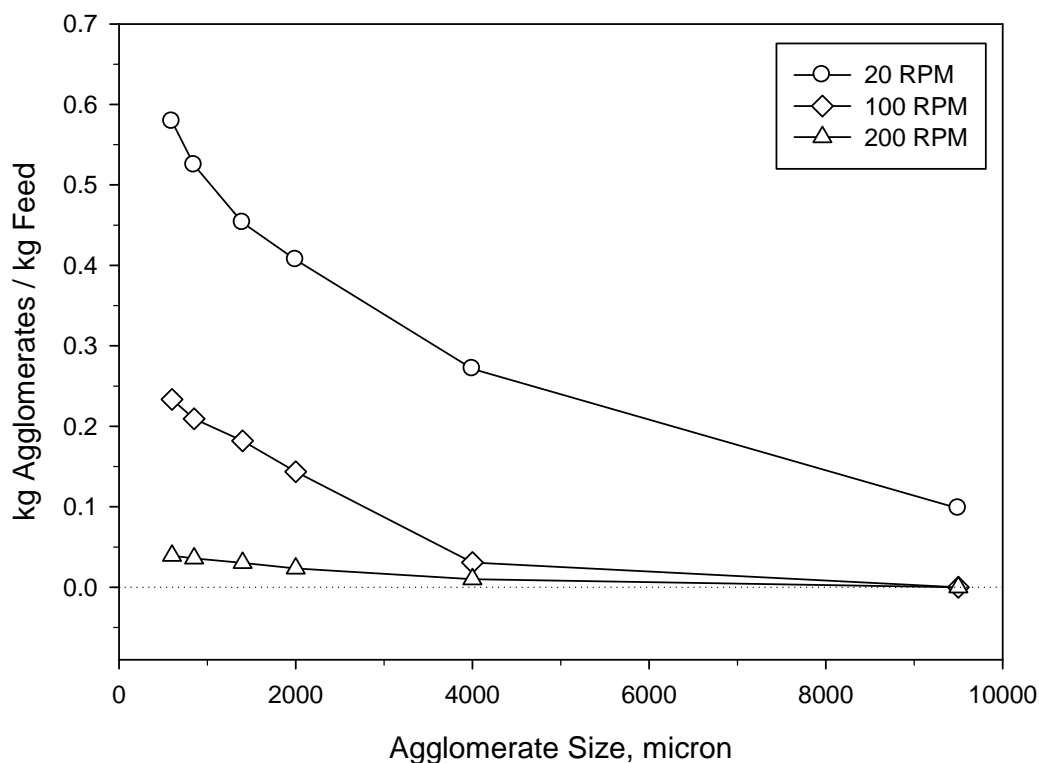
Figure 2-5 - Impact of mixing on cumulative agglomerate distributions (reactor temperature = 530 °C; error bars represent one standard deviation)

Figure 2-5 demonstrates the impact of mechanical agitation on the cumulative mass of agglomerates greater than 600 µm at varying agitator speeds. Increasing the speed of agitation from 20 to 100 RPM resulted in a 60 wt% reduction in total agglomerates, while increasing to 200 RPM resulted in a 93 wt% reduction. Agglomerates larger than 4000 µm were essentially eliminated at 200 RPM, with very limited numbers of small

agglomerates surviving. The survival of small agglomerates under these conditions is understandable, given that the geometry of the mixer blade allowed for solids to be forced towards the center of the bed instead of being crushed against the reactor wall.

Figure 2-6 demonstrates the increase of agglomerates at each size cut with respect to ideal conditions at 200 RPM. If the 200 RPM condition is deemed the ideal case of a well-mixed system, a reduction in mixing to 100 RPM increases the survival chances of small agglomerates, while large agglomerates are not overly common. A further reduction in mixing speed to 20 RPM drastically increases the amount of small agglomerates that are capable of surviving but, more importantly, the slow movement of the mixer blade allows for large agglomerates to bypass the blade and continue to survive. If these large agglomerates survive in the reactor, the mass and heat transfer limitations imposed by the large size hinder quick reaction rates and vaporization of the liquid. As a result, there was a higher likelihood of coking side reactions occurring during the poorly mixed 20 RPM case.
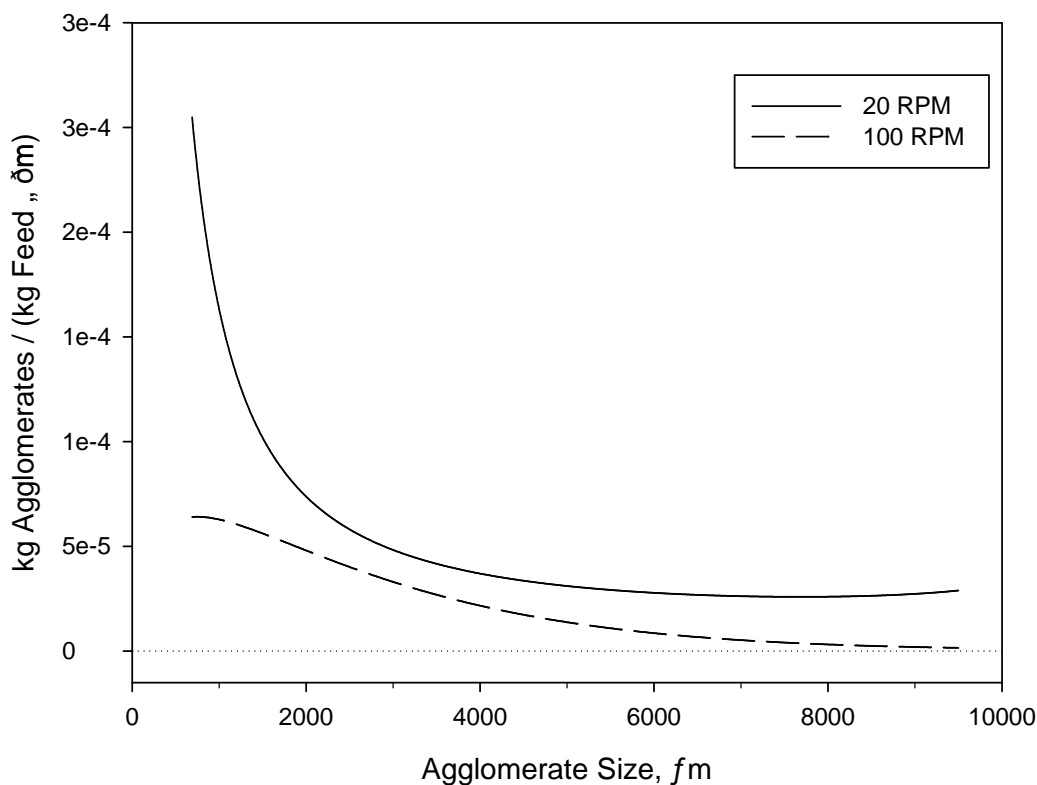
Figure 2-6 - Agglomerate distribution deviations from ideal conditions

2.3.2   Short Vapor Phase Residence Time

Coke yield decreased significantly as agitator speed was increased. Figure 2-7 indicates that, under poorly mixed conditions at 20 RPM, the coke yield was 27 wt%. As mixing was improved within the reactor, a coke yield of 23 wt% was achieved. A positive correlation has been found between the cumulative mass of agglomerates above 600 µm and the coke yield. The reduction in coke yield can be attributed to agglomerate breakage resulting in quicker reaction of the bitumen feed and vaporization of the product compounds, which are later condensed as liquid oil product. The probability that the differences between the data sets can be attributed to random error is only 3 % for the 20 and 100 rpm sets (p_{20-100} = 0.03) and 22 % for the 100 and 200 rpm sets ($p_{100-200}$ =0.22).

Figure 2-7 - Effect of mixing on coke yield at short vapor residence time (reactor temperature = 530 °C; vapor phase residence time = 4.9 s; p_{20-100} = 0.03; $p_{100-200}$ =0.22)

Experiments conducted under short vapor residence time indicated an increase in liquid yield with mixing, as seen in Figure 2-8. An increase of approximately 3 wt% was found between the 20 and 100 RPM case, with a further increase of 1 wt% when mixing was increased to 200 RPM. A statistical comparison of means between the data sets indicated that there was a significant increase in liquid yield between 20 and 100 RPM. Between

100-200 RPM, the slight scatter in the results reduced the statistical probability associated with the slight increase in liquid yield. Given the difference in liquid yield between the 100 and 200 RPM cases, is likely that the critical RPM, above which the liquid yield would not be affected by any further increase in mixing speed, was slightly above 100 RPM. The maximum liquid yield obtained in this process was about 73 wt%.

Figure 2-8 - Effect of mixing on liquid yield at short vapor residence time (reactor temperature = 530 °C; vapor phase residence time = 4.9 s; $p_{20-100} = 0.13$; $p_{100-200} = 0.30$)

It has been found that there was a negative correlation between the cumulative mass of agglomerates above 600 µm and liquid yield at short vapor residence times. Essentially, as agglomerates are broken up by mechanical agitation, the liquid trapped in the agglomerates is released and dispersed across the surface of smaller fragments, resulting in reduced mass and heat transfer limitations. This leads to increased vaporization of the thermal cracking products, leading to an increased liquid yield at short vapor residence time. At 100 and 200 RPM, agglomerates above 9500 µm have been eliminated, 4000-9500 µm agglomerates have been drastically reduced, and small agglomerates are found in fewer numbers. The reduction in large agglomerates was significant when the RPM was increased from 20 to 100 RPM. It was also observed that the majority increase in the

liquid yield occurs over this same RPM range. Together, these results indicate that the breakage of large agglomerates was responsible the increased liquid yields, as it allowed for a faster reaction rate and reduced likelihood of-coking reactions.

It was evident that there was no impact of bed mixing on gas yields under short residence times (Figure 2-9). Gas yields under these conditions were approximately 5 wt% for all mixing conditions, and statistical analysis indicates there was no effect of mechanical agitation over the range of tested values. Coupled with the increased liquid yield over the same operating conditions, it appears as if agglomerate breakage was only responsible for increased liquid products under short residence times, and the liquid released from the agglomerates did not spend sufficient time in the vapor phase to continue to crack to gas.

Figure 2-9 - Effect of mixing on gas yield at short vapor residence time (reactor temperature = 530 °C; vapor phase residence time = 4.9 s; p_{20-100} = 0.53; $p_{100-200}$ = 0.69)

The reduction in coke yield and subsequent increase in liquid yield are in agreement with the findings of Chaudhari (2012). However, that investigation found a 12 wt% reduction in coke yield using heavy crude oil and sand, considerably greater than the 4 wt% reduction found using bitumen (Figure 2-7). Correspondingly, the liquid yield increases found with heavy oil were significantly larger than with the bitumen system. Finally, the

heavy oil system found gas yields increases of up to 5 wt% under comparable temperature and vapor residence times, which are in direct contradiction with the above results using bitumen (Figure 2-9). The discrepancies between the results is most likely attributed to the differences in feedstock and bed material (Chaudhari, 2012)
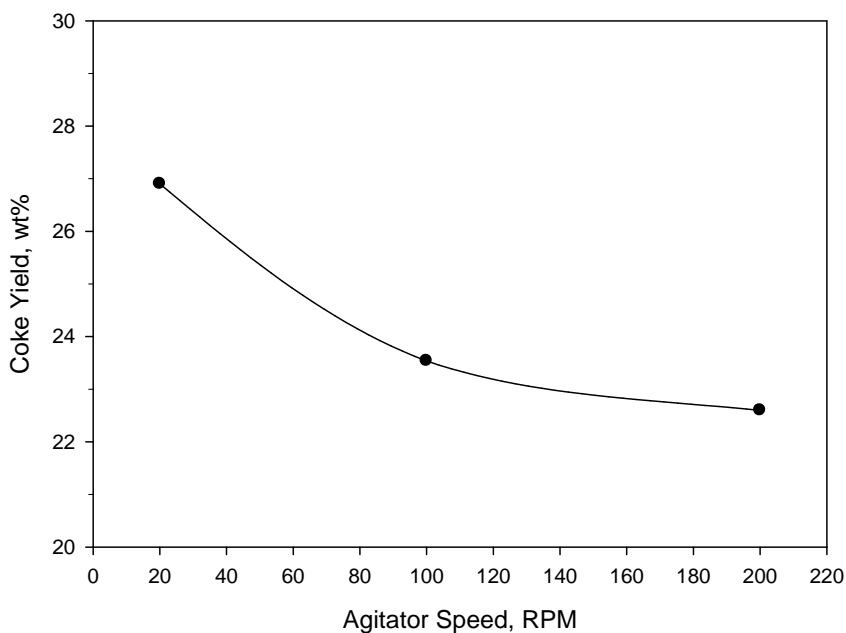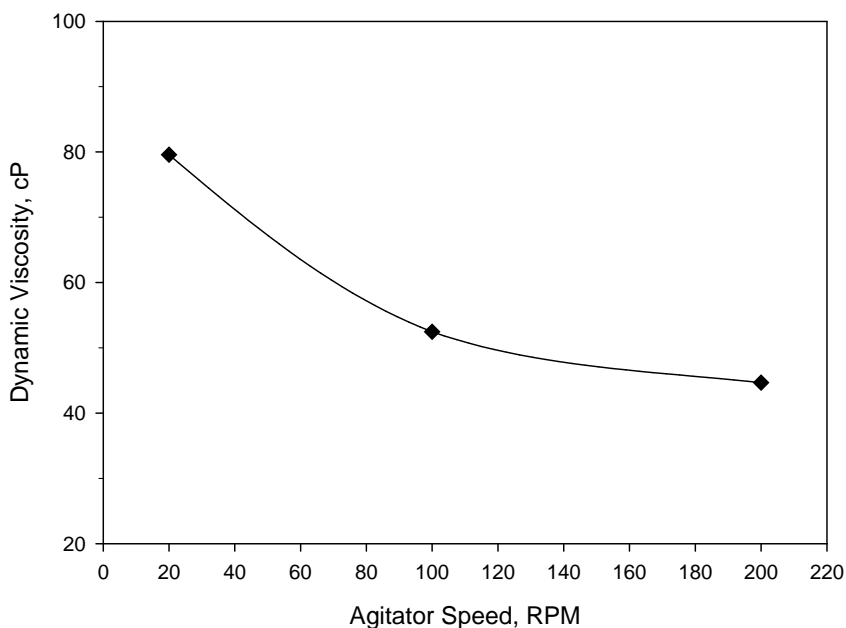

Figure 2-10 - Impact of mixing on viscosity at short vapor residence time (reactor temperature = 530 °C; vapor phase residence time = 4.9 s; $p_{20\text{-}100}$ = 0.00; $p_{100\text{-}200}$ = 0.06)

Product oil analysis was conducted in order to determine the extent of thermal cracking. Figure 2-10 highlights the impact of applied mixing on product oil dynamic viscosity at short vapor residence times. It has been found that as mixing levels were increased there was a statistically significant decrease in viscosity. This trend can be found from 20-100 RPM as well as 100-200 RPM. Combined with agglomerate breakage and the increase in liquid yield that has been established (Figure 2-8), it can be concluded that the liquid released from agglomerates produced a liquid product which had a lower viscosity than the bulk of the liquid that was produced during the normal coking process.
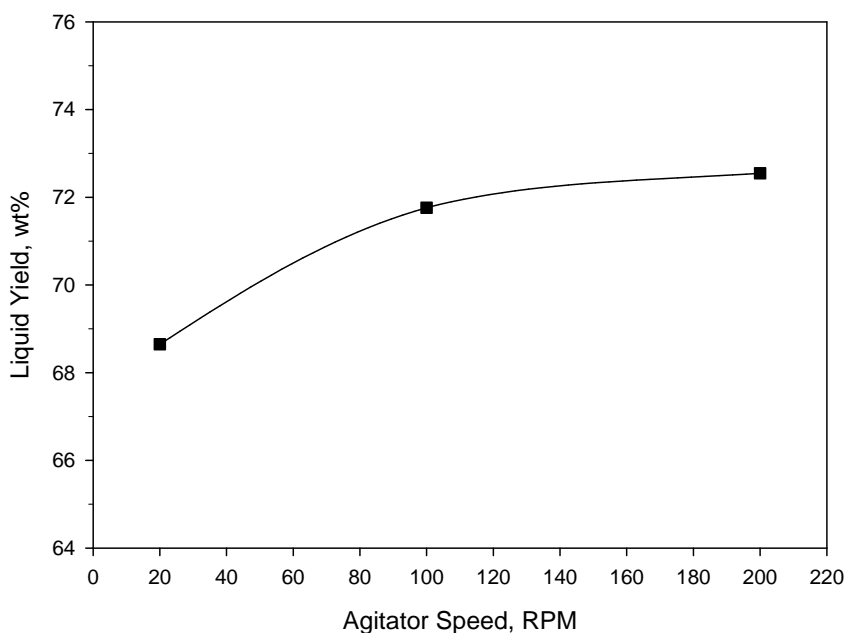
Figure 2-11 - Impact of mixing on molecular weight at short vapor residence time (reactor temperature = 530 °C; vapor phase residence time = 4.9 s; p_{20-100} = 0.14; $p_{100-200}$ = 0.09)

Figure 2-11 shows the impact of mixing on average molecular weight at low vapor residence times. The liquid released from agglomerates had a lower molecular weight than the bulk liquid produced during poorly-mixed conditions, enough so to shift the molecular weight distribution. That is, by quickly removing liquid from the agglomerates, it is possible to produce liquid of a lower viscosity and lower molecular weight. It appears as though the liquid initially trapped in agglomerates was more reactive once it had been released and dispersed among the rest of the bed. This higher reactivity would result in an increased likelihood of the compounds undergoing cracking reactions to product less viscous, lower-molecular weight compounds. This corroborates well with the increased liquid yield and decreased coke yield, as the compounds released from the agglomerates crack into light vapor products instead of continuing to produce coke from side reactions within the larger agglomerates.

2.3.3   Long Vapor Phase Residence Time

Coke yields at prolonged vapor residence times corroborate very well with the yields obtained at short residence times, as is expected (Figure 2-12). It has been found that coke yield decreases with agitation at both residence times, as is indicated from the agglomerate distributions shown in Figure 2-5. The majority of the coke yield reduction was found to occur from 20-100 RPM, while the reduction between 100-200 RPM was minimal by comparison. As agitation was increased to 200 RPM, coke yields of 23 wt% were attained.

Figure 2-12 - Effect of mixing on coke yield at long residence time (reactor temperature = 530 °C; vapor phase residence time = 10.6 s; p_{20-100} = 0.01; $p_{100-200}$ = 0.40)

Figure 2-13 demonstrates the impact of agitator speed on liquid yields at long vapor phase residence times. It is evident that the liquid yield decreased as the residence time increased, as is expected. The liquid yield was approximately 63 wt% at the longer residence time, a reduction of 6 wt% when compared to the liquid yield at the short residence time. This indicates that longer vapor residence times promote further vapor phase cracking reactions which convert part of the liquid product into gas.

Figure 2-13 - Effect of mixing on liquid yield at long vapor residence time (reactor temperature = 530 °C; vapor phase residence time = 10.6 s; p_{20-100} = 0.16; $p_{100-200}$ = 0.31)
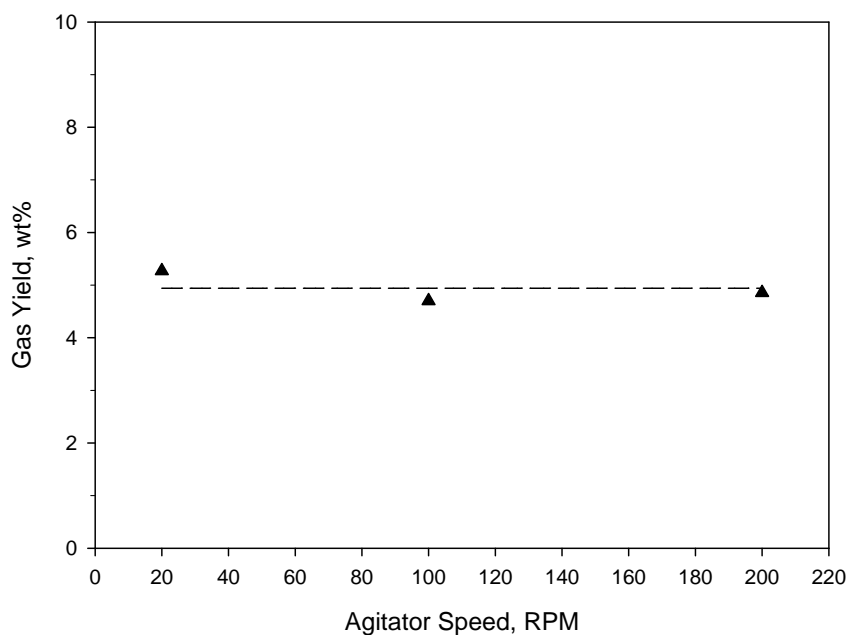

Figure 2-14 - Effect of mixing on gas yield at long vapor residence time (reactor temperature = 530 °C; vapor phase residence time = 10.6 s; p_{20-100} = 0.01; $p_{100-200}$ = 0.49)

Figure 2-13 shows that increased bed agitation had an impact on liquid yield at both long and short residence times, although the increase in liquid yield at the longer vapor phase residence time was less than the increase observed at the short vapor residence time. This can be attributed to the prolonged residence time allowing for increased vapor cracking reactions compared to the short residence time, as liquids are being released from agglomerates and being lost to the gas phase before being condensed and collected.

The effect of bed mixing on gas yield is illustrated Figure 2-14. It has been found that gas yield increased as agitator speed increased. However, this has only been found at prolonged residence times. At poorly mixed conditions at 20 RPM the average gas yield was 10.2 wt%, which increased by 2.5% when agitation was applied. At prolonged residence times secondary vapor phase cracking reactions continue in the heated tube reactor, which was maintained at the same temperature as the MFR. This results in the cracking of lighter liquid products to produce non-condensable gases. This corroborates well with previous data on increased liquid yields. Statistical analysis on gas yields gives a 99% probability of increased gas yield as a result of increased bed mixing between 20 100 RPM. The 100 and 200 RPM cases are essentially identical. In addition, it was observed that gas yields are, overall, higher at prolonged residence times than short residence times. This occurs at poorly mixed and well-mixed conditions. The increase can be attributed to the vapor cracking reactions converting both bulk liquid produced during coking as well as liquid released from agglomerates.

The comparison between the results obtained at the two residence times suggests that increasing agitation reduces the production of coke (Figure 2-12) and increases the production of lighter vapors (Figures 2-9, 2-10 and 2-11). These lighter vapors are more susceptible to vapor phase cracking, increasing the production of gas at the long residence time (Figure 2-14).
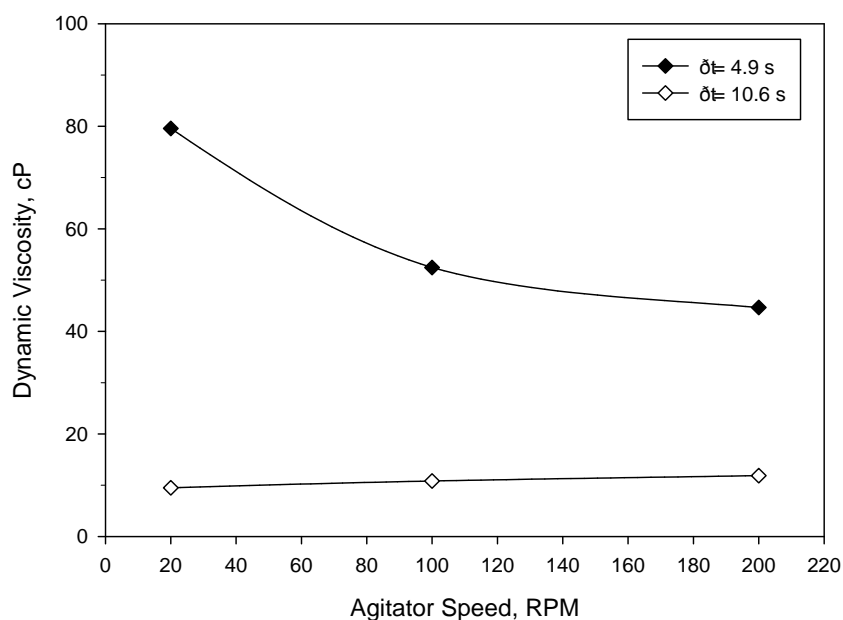
Figure 2-15 - Impact of mixing on viscosity at long residence time (reactor temperature = 530 °C; vapor phase residence time = 10.6 s; $p_{20\text{-}100}$ = 0.01; $p_{100\text{-}200}$ = 0.01)
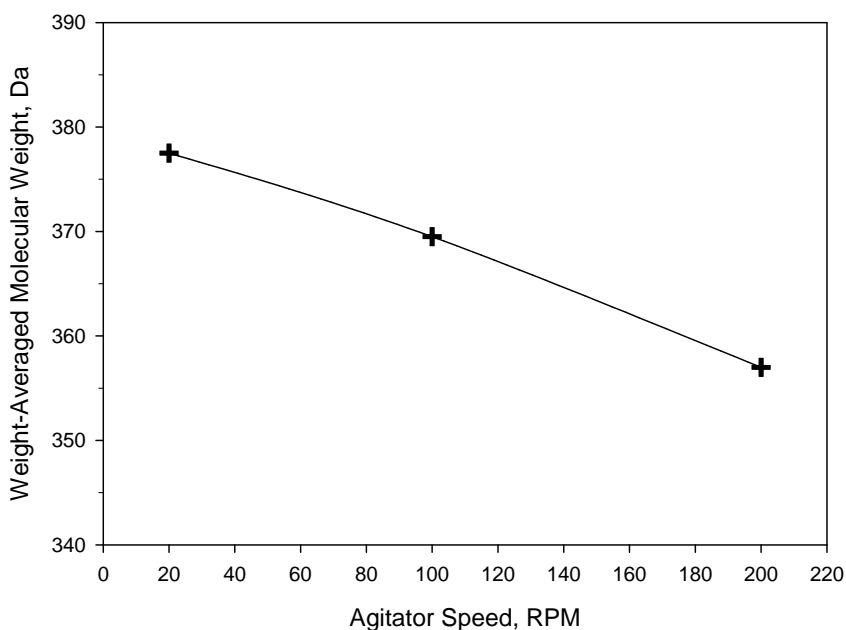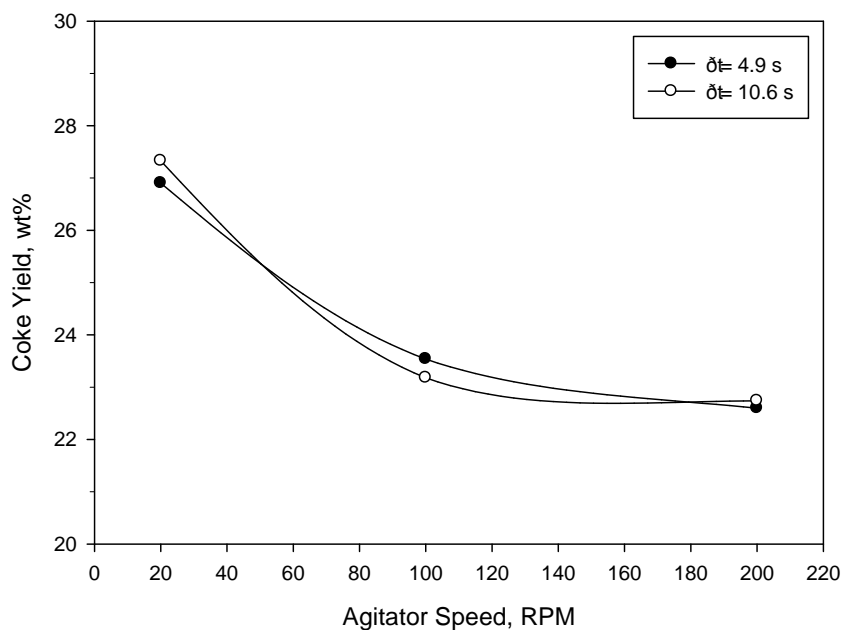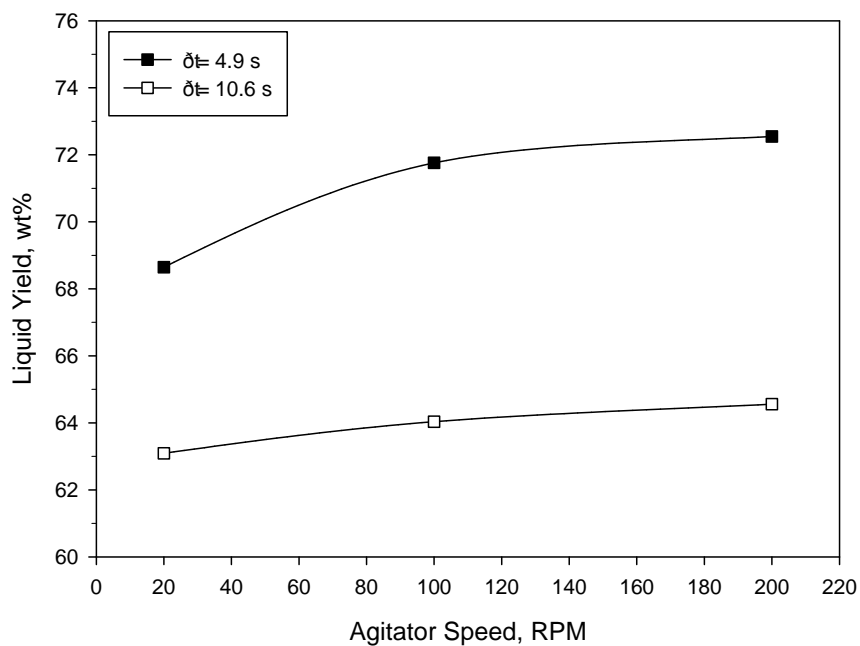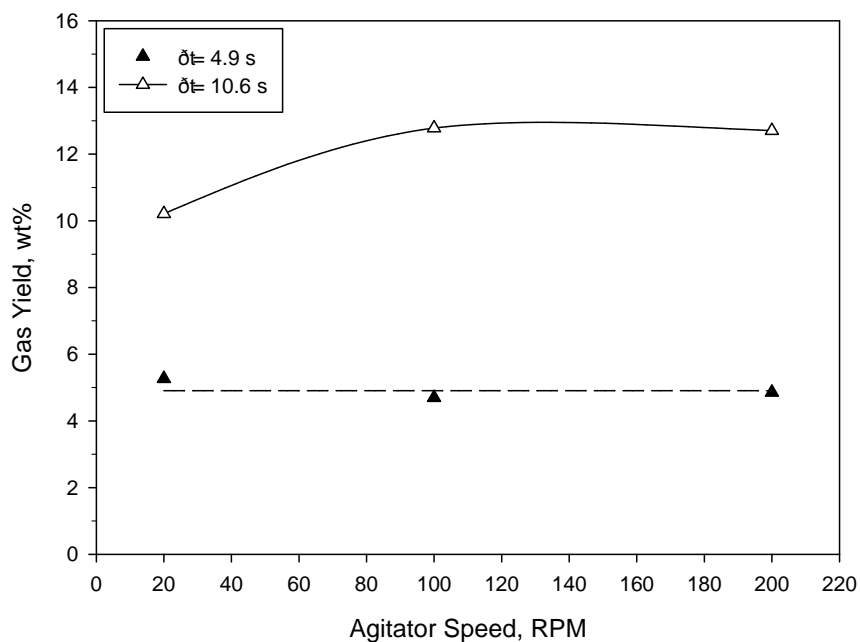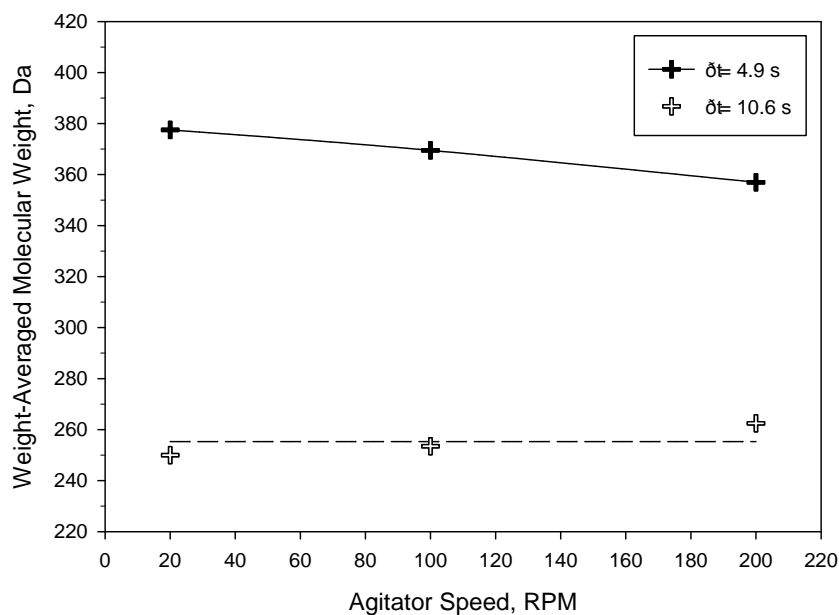

Figure 2-16 - Impact of mixing on molecular weight at long residence time (reactor temperature = 530 °C; vapor phase residence time = 10.6 s; $p_{20\text{-}100}$ = 0.38; $p_{100\text{-}200}$ = 0.21)

An interesting trend developed at prolonged residence times. As depicted in Figure 2-15, product oil viscosity increased with applied bed mixing. Oil viscosity was determined to be in the range of 9.5 to 11.9 cP at 60 for all cases. However, comparison of means between the data sets indicates conclusively that viscosity was increased as a result of mechanical agitation. Taking previous results into consideration, it is evident that the increased viscosity was a result of heavier fractions of oil being concentrated in the liquid phase. At prolonged residence times, the reduction in agglomerates resulted in slight increases in liquid yields, while liquids continued to crack to the gas phase. Experimentation at shorter residence times indicated that the liquid released from agglomerate fracture was more reactive than the bulk liquid produced during the course of normal injection and coking. It can then be concluded that the liquid released from the agglomerates were more reactive and cracked to gas, alongside some of the liquid produced over the course of normal injection. Due to this vapor phase cracking of lighter fractions, more viscous liquid products were concentrated in the liquid phase, leading to an overall increase in liquid product viscosity. In addition, the viscosity of product oil at prolonged vapor phase residence times was lower than that of short residence, due to the vapor phase cracking reactions that continued to reduce the viscosity of the product oil.

Figure 2-16 demonstrates that the molecular weight of the liquid product was significantly reduced at long vapor residence times compared to short residence times. This can be attributed to the vapor phase cracking reactions which convert higher molecular weight compounds into lower molecular weight compounds. It has also been found that molecular weight experienced slight increases with mixing. However, the statistical probabilities of these trends were not as high as that of viscosity. Given the reproducibility of molecular weight analysis, it can be concluded that mixing does not have a significant impact on molecular weight distributions at prolonged vapor residence times as the effects are dampened by the impact of vapor phase cracking.

2.3.4 Statistical Significance

Table 2-3 highlights the statistical significance of the previous results. It was found that prolonged vapor phase residence time had a significant impact on liquid and gas yield. It can then be concluded that as vapor residence time was increased there was a significant reduction in liquid yields, with a corresponding increase in gas yields. It is also possible to conclude that both viscosity and molecular weight were decreased as a result of prolonged vapor phase residence time. Note that the statistical probability of these results are 95 % and above, and are validated at all levels of mechanical agitation that have been tested. In addition, it has been demonstrated that there was essentially no impact of residence time on coke yields, as is expected.

Table 2-3 - Effect of residence time

	Impact of Prolonged Residence Time	p-value at 20 RPM	p-value at 100 RPM	p-value at 200 RPM
Liquid Yield	Decrease	0.02	0.00	0.05
Gas Yield	Increase	0.04	0.00	0.02
Viscosity	Decrease	0.00	0.00	0.00
Molecular Weight	Decrease	0.02	0.00	0.01
Coke Yield	Two-tailed	0.70	0.74	0.93

Table 2-4 indicates the statistical significance of mixing effects at short and long residence times. It is important to note that the effects of mixing had a higher probability of impacting yields and product quality between 1-200 RPM, with reduced probabilities between 100-200 RPM. This can be attributed to the critical mixing level being in the range of 100-200 RPM, beyond which the impact on yields and product quality was minimal. However, when performing a comparison between the poorly mixed case at 20 RPM to the well-mixed case at 200 RPM, applied bed mixing had a higher probability of impacting yields and quality. At short residence times it was determined that mixing did not impact gas yields. However, increasing bed mixing from 20 to 200 RPM had a statistically significant increase in liquid yield, while product oil viscosity and molecular weight were reduced under these conditions. These impacts had a minimum of 95 % probability of being attributed to the effects of mixing.

Table 2-4 - Effect of mixing

	Impact of Mixing	p-value over the range of 20-100 RPM	p-value over the range of 20-200 RPM
Short Residence Time:			
Liquid Yield	Increase	0.13	0.05
Gas Yield	Two-tailed	0.53	0.61
Viscosity	Decrease	0.00	0.01
Molecular Weight	Decrease	0.14	0.02
Long Residence Time:			
Liquid Yield	Increase	0.16	0.14
Gas Yield	Increase	0.01	0.07
Viscosity	Increase	0.01	0.00
Molecular Weight	Increase	0.38	0.19
Average of Residence Times:			
Coke Yield	Decrease	0.00	0.00

The impacts of bed mixing had a slightly reduced probability of occurring at the prolonged vapor residence time (Table 2-4). Between the range of 20-200 RPM, it was found that improved mixing resulted in statistically significant increases in gas yields and product oil viscosity. These increases had a minimum of 93 % probability of being attributed to the effects of mixing. Although there appeared to be increases in liquid yield and molecular weight at long residence times, the simultaneous impact of vapor phase cracking introduced a degree of uncertainty as to whether these mixing effects were significant under these conditions. These increases had a minimum of 81 % probability of being attributed to mixing. As it has been previously been established that vapor residence time does not impact coke yields, these data sets have been merged to gain a more accurate determination of the impacts of mechanical agitation. It can be concluded that increases in applied bed mixing reduced the coke yield in the reactor set-up used in this study.

2.4 Conclusions

The Mechanically Fluidized Reactor has been successfully developed and implemented for Fluid Coking€ applications. It has been determined that multiple vapor phase residence times can be investigated simultaneously while reducing intrinsic errors present in a complex system such as coking. The impact of applied bed mixing and vapor phase cracking have been investigated to determine their impact on Fluid Coking yields, as well as quantification of their impact on product oil quality.

It has been found that bed mixing was responsible for agglomerate breakage and had the capacity to reduce the cumulative mass of agglomerates within the reactor. In addition, agglomerate breakage has been found to reduce coke yields due to the release of liquid feed that has been trapped. Agglomeration within cokers causes the entrapment of liquid feed, resulting in reduced liquid yields due to the mass and heat transfer limitations of larger wet agglomerates. Agglomerate breakage and subsequent liquid dispersion results in increased yields of low-viscosity, low-molecular weight liquid at short vapor residence times.

However, the liquid released from agglomerates was more reactive and continued to crack to gas at long vapor phase residence times, resulting in concentration of higher viscosity, higher-molecular weight compounds in the liquid phase. This study highlights the importance of quick agglomerate breakage and feed dispersion in fluid cokers by relating agglomerate destruction to the quantity and quality of liquid product that can be attained.

2.5   References

Ali, M., Courtney, M., Boddez, L., & Gray, M. (2010). Coke Yield and Heat Transfer in Reaction of Liquid–Solid Agglomerates of Athabasca Vacuum Residue. The Canadian Journal of Chemical Engineering, 88(1), 54.

Aminu, M. O., Elliott, J. A. W., McCaffrey, W. C., & Gray, M. R. (2004). Fluid Properties at Coking Process Conditions. Industrial & Engineering Chemistry Research, 43(12), 2929–2935.

Ariyapadi, S. (2004). Interaction Between Horizontal Gas–Liquid Jets and Gas–Solid Fluidized Beds. The University of Western Ontario.

Ariyapadi, S., Holdsworth, D. W., Norley, C. J. D., Berruti, F., & Briens, C. (2003). Digital X-ray Imaging Technique to Study the Horizontal Injection of Gas–Liquid Jets into Fluidized Beds. International Journal of Chemical Reactor Engineering, 1.

Chaudhari, M. (2012). Effect of Liquid–Solid Contact on Thermal Cracking of Heavy Hydrocarbons in a Mechanically Fluidized Reactor. The University of Western Ontario.

Darabi, P., Pougatch, K., Salcudean, M., & Grecov, D. (2010). Agglomeration of Bitumen-Coated Coke Particles in Fluid Cokers. International Journal of Chemical Reactor Engineering, 8.

Gray, M. R. (2002). Fundamentals of Bitumen Coking Processes Analogous to Granulations : A Critical Review. The Canadian Journal of Ch 80(June), 393–401.

Gray, M. R., Le, T., McCaffrey, W. C., Berruti, F., Soundararajan, S., Chan, E., ƒ Thorne, C. (2001). Coupling of Mass Transfer and Reaction in Coking of Thin Films of an Athabasca Vacuum Residue. Industrial & Engineering Chemistry Research, 40, 3317–3324.

Gray, M. R., Le, T., & Wu, X. A. (2007). Role of Pressure in Coking of Thin Films of Bitumen. The Canadian Journal of Chemical Engineering, 85(October), 773.

Gray, M. R., McCaffrey, W. C., Huq, I., & Le, T. (2004). Kinetics of Cracking and Devolatilization during Coking of Athabasca Residues. Industrial & Engineering Chemistry Research, 43(18), 5438–5445.

Gray, M. R., Zhang, Z., McCaffrey, W. C., Huq, I., Boddez, L., Xu, Z., & Elliott, J. a. W. (2003). Measurement of Adhesive Forces during Coking of Athabasca Vacuum Residue. Industrial & Engineering Chemistry Research, 42(15), 3549.

Hammond, D. G., Lampert, L. F., Mart, C. J., Massenzio, S. F., Phillips, G. E., Sellards, D. L., & Woerner, A. C. (2003). Review of Fluid Bed Coking Technologies (pp. 1–8).

House, P. K., Saberian, M., Briens, C. L., Berruti, F., & Chan, E. (2004). Injection of a Liquid Spray into a Fluidized Bed: Particle–Liquid Mixing and Impact on Fluid Coker Yields. Industrial & Engineering Chemistry Research, 43, 5663–5669.

McCaffrey, D. S., Hammond, D. G., & Patel, V. R. (1998). Fluidised Bed Coking Utilising Bottom of the Barrel (pp. 1–7).

Pfeiffer, R. W., Borey, D. S., & Jahnig, C. E. (1959). Fluid Coking of Heavy Hydrocarbons. United States: United States Patent Office.

Salman, A. D., Fu, J., Gorham, D. ., & Hounslow, M. . (2003). Impact Breakage of Fertiliser Granules. Powder Technology, 130(1), 359–366.

Sanchez, F. J., & Granovskiy, M. (2013). Application of radioactive particle tracking to indicate shed fouling in the stripper section of a fluid coker. The Canadian Journal of Chemical Engineering, 91(6), 1175–1182.

Speight, J. G. (1998). Petroleum Chemistry and Refining. Washington: Taylor & Francis.

Teare, M., Cruickshank, R., Miller, S., Overland, S., & Marsh, R. (2014). Alberta‚s Energy Reserves 2013 and Supply/Demand Outlook 2014-2023. Calgary.

Weber, S., Briens, C., Berruti, F., Chan, E., & Gray, M. (2008). Effect of Agglomerate Properties on Agglomerate Stability in Fluidized Beds. Chemical Engineering Science, 63(17), 4245–4256.

Weber, S. (2009). Agglomerate Stability in Fluidized Beds. University of Western Ontario.

Chapter 3

3 Effects of Bed Mixing and Vapor Residence Time on Bitumen Thermal Cracking

3.1 Introduction

The Fluid Coking® process is utilized to convert heavy residues into lighter distillates, which can then fractionated and upgraded separately into transportation fuels, or blended to produce a synthetic crude oil for further refining (McCaffrey, Hammond, & Patel, 1998; Speight & Ozum, 2002). This non-catalytic process utilizes a fluidized bed of hot petroleum coke to thermally crack bitumen feed into vapor and gas, while concentrating impurities in a solid coke product. Within the Fluid Coker, the injection of the liquid feed results in the formation of liquid-solid agglomerates. Poor liquids injection and agglomerate formation is detrimental to reactor performance, leading to increased yields of petroleum coke at the expense of valuable liquids (Gray, 2002; House, Saberian, Briens, Berruti, & Chan, 2004; Sanchez & Granovskiy, 2013). Detailed descriptions of the Fluid Coking process and operating parameters can be found in Chapter 1.

Several authors have reported the impact of agglomerate properties (Ali et al., 2010; Salman et al., 2003; Weber et al., 2008; Weber, 2009) as well as bitumen film thickness (Aminu et al., 2004; Gray et al., 2001, 2003, 2007) on cracking reactions. These results indicate that agglomerate survival leads to entrapment of feed liquid and mass and heat transfer limitations which allow for retrograde reactions to convert feed liquid into coke. In addition, agglomerate breakage disperses liquid feed across the surface of individual particles, leading to a reduction in mass and heat transfer limitations and faster cracking reaction rates. A more in-depth discussion of agglomerate formation and breakage can be found in Chapter 1.

The main objective of this study is to investigate the impacts of applied bed mixing and vapor phase cracking on the Fluid Coking® of vacuum topped bitumen in a traditional fluidized bed. In particular, this study aims to develop an understanding of the impact of bed mixing on agglomerate distributions as this is an area of limited study. It is crucial to

determine the impact of increased agitation independently of other effects: instead of increasing the fluidization velocity, which improves mixing but also reduces the vapor residence time and the vapor partial pressure, the study uses mechanical agitation to enhance mixing at constant fluidization velocity.

3.2 Experimental

3.2.1 Materials

Thermal cracking reactions were carried out using Athabasca vacuum topped bitumen provided by Syncrude Canada Ltd. This feed represents the distillable residue remaining after atmospheric and vacuum distillation. The feedstock had a specific gravity of approximately 1.01. Molecular weight analysis indicated that the feed had a weight-averaged molecular weight of 1945 g/mol. Ultimate elemental analysis is reported in Table 3-1.

Nitrogen was utilized as fluidization, atomization, and make up gas in order to obtain an oxygen-free environment suitable for thermal cracking reactions. The fluidized was composed of petroleum coke having a particle density of 1450 kg/m^3 and a Sauter mean diameter of 140 …m. Total bed mass was held constant at 0.800 kg for each experiment. In order to maintain consistent bed conditions over the course of experimentation, bed coke samples were analyzed in a Sympatec Helos/BF Particle Size Analyzer prior to experimentation.

Table 3-1 - Bitumen specifications

Ultimate Elemental Analysis:		
Carbon	82.1	wt%
Hydrogen	9.8	wt%
Nitrogen	0.6	wt%
Sulphur	5.3	wt%
Oxygen (by difference)	2.2	wt%
Weight-Averaged Molecular Weight	1945	g/mol
Specific Gravity	1.06	

3.2.2   Experimental Apparatus

Experiments were conducted in a pilot-scale Fluid Coking Reactor (FCR) shown in Figure 3-1. The pilot-scale system consists of a cylindrical fluidized bed reactor with an internal diameter of 0.076 m and a total height of 0.594 m. The unit was operated at atmospheric pressure with operating temperatures of 510 and 530 °C. Vapour residence times were controlled through the addition of freeboard extensions onto the top of the reactor. These extensions have an internal diameter of 0.128 m and a height varying from 0.277 m to 0.86 m. Freeboard extensions allowed for vapour-phase residence time to be manipulated through freeboard volume instead of gas flowrate, which facilitated consistent bed hydrodynamics over the course of experimentation.

Figure 3-1 - ICFAR Fluid Coking reactor

The reactor was equipped with ten Watlow mica electric band heaters covering the reactor and extensions. Fluidization and atomization gases were preheated using Omega AHP-3742 in-line air heaters. Fluidization gas was maintained at 350 $^{\circ}$C while atomization gas was held at 220 $^{\circ}$C. Reactor temperature control was accomplished using fourteen type K thermocouples, with accompanying Honeywell UDC200 Mini-Pro Digital controllers. In addition, temperature monitoring was provided for the bitumen feed and vapor exit lines.

Figure 3-2 - Fluid Coking Reactor mixer assembly

Fluidizing gas was injected at the base of the reactor through a perforated plate design consisting of ten porous disks. The porous disks are arranged in a ring at the base of the mixer driveshaft (Figure 3-2) and have a pore size of 40 μm. Atomization gas entered at the injection nozzle located 0.10m above the distributor. Make-up gas was injected above the distributor plate to provide the necessary volumetric gas flowrate to assist in controlling the residence times of the reactor. The mixing system was mounted on the bottom of the reactor, with the driveshaft located in the center of the reactor flange (Figure 3-2). The mixer blade was driven by an electric variable speed motor, allowing

for mechanical agitation speed ranging from 0 to 200 RPM. The injection nozzle penetration in this reactor prevented the mixer blade from being oriented to scrape the reactor wall, as this would have resulted in severe nozzle damage. As such, the mixer blade has been retracted by approximately 0.015 m to accommodate the injection nozzle

3.2.3   Experimental Procedure

Bitumen was fed to the reactor through the use of a dual-piston pump. Bitumen was preheated to a temperature of approximately 120-125 °C in the top chamber of the pump. Hydraulic oil was pumped into the bottom chamber at a constant flowrate, forcing the piston upwards. This pressurized the bitumen chamber and displaced the oil into the injection line at a constant flowrate. The injection line was maintained at a temperature of approximately 200 °C.

Injection was accomplished via a two-phase feed nozzle modified from Ariyapadi et al. (2003). The details of the feed nozzle are provided elsewhere (Ariyapadi et al., 2003). Bitumen was injected through the central tube, while atomization nitrogen was passed through the annular region. The liquid injection tube had been advanced to extend beyond the exterior jacket in order to accomplish external mixing. The liquid tube extends around 2.0 mm from the jacket, with the nozzle penetrating approximately 0.01 m into the reactor bed. Atomization gas was preheated to a temperature of approximately 200 °C. At the tip of the nozzle, bitumen was forced through a 0.1 mm diameter nozzle tip, and atomization gases from the nozzle jacket dispersed the feed into a fine spray.

As the bitumen was sprayed into the reactor, it interacted with the bed coke particles to form wet agglomerates, some of which broke apart due to shear forces from gas bubbles. The bitumen thermally cracked to lower molecular weight products, which vaporized and deposited a layer of fresh coke on the original bed coke particles. The product vapors travelled up the reactor and freeboard extensions before exiting through the hot filter. The product line exiting the reactor was maintained at 200 °C using a double-pipe heat exchange with heated air. This temperature has been found sufficient to reduce secondary reactions, while eliminating backpressure issues caused by vapor product condensation.

Figure 3-3 - FCR process diagram

Immediately after the reactor were two cyclonic condensers in series, immersed in an ice water bath. Heavy fractions of the oil were collected in the bottom of the condensers, while non-condensable gases and entrained mist continued downstream to an electrostatic precipitator. Within the ESP, a voltage of 15 kV was applied between the electrode and ESP wall, resulting in ionization of the gas around the electrode through corona discharge. The entrained mist exiting the ESP was charged by the ionized gas, and the electric field around the electrode forced the charged mist to the wall. Mist condensed on the wall and drained to the bottom of the ESP for collection. The non-condensable gases continued through a cotton filter and were sampled for subsequent gas analysis. Finally, the exhaust gas was vented to atmosphere.

The mass change of the condensers, electrostatic precipitator, and filter were used to determine the liquid yield. Gas composition data and nitrogen flowrates were used to determine the gas yield. Coke yield was first estimated from the mass change of the reactor bed. Due to slight variability in bed material volatiles content, the coke yields are reported by difference to provide more accurate determination of the impacts of mechanical agitation.

Table 3-2 - FCR operating conditions

		Shorter Vapor Residence Time	Longer Vapor Residence Time
Bed Residence Time	s	1.2	1.2
Vapor Phase Residence Time	s	5.3	13.0
Total Residence Time	s	6.5	14.2
Injection Rate	mL/min	5.7	
Injection Time	min	20	
Reactor Temperature	°C	530 ± 8	
Reactor Pressure	psig	0	
Fluidization Velocity	m/s	0.08	

Bitumen was preheated to a temperature of approximately 120 °C in a double-piston pump and injected at a rate of 5.7 mL/min. Injection was continuous over the course of 20 minutes in order to obtain the sample volumes required for analysis and reduce

measurement errors. The reactor temperature was maintained at 530°C unless otherwise specified. The experimental procedure was as follows:

1. Experimentation was initially conducted at a gas-liquid ratio (GLR) of 105 wt% and a long vapor residence time of 13.0 seconds. Injection was performed with and without mechanical agitation.
2. Experimentation was then performed at a GLR of 105 wt%, and a short vapor phase residence time of 5.3 seconds. Injection was performed with and without mechanical agitation.
3. The impact of reduced GLR was carried out using GLR values of 2 and 8.0 wt%. The vapor phase residence time was maintained at 5.3 seconds, and injection was carried out with and without mechanical agitation.
4. Injection was then performed at a reduced temperature of 510°C and a GLR of 105 wt%.

Experimentation was initially performed at a temperature of 530°C using a bed drying period of 20 s after injection was stopped. It was then determined that a 20 s drying period was not sufficient to completely dry out the bed under the poorly mixed conditions at 0 RPM, as there were still minute quantities of unvaporized liquid trapped in the larger agglomerates. A drying time of 20 minutes was then used to determine the true liquid and coke yields under the poorly mixed condition. As such, the reported values for the 0 RPM conditions represent the true liquid and coke yields with 20 minutes of bed drying.

Statistical analysis using replicate experiments has been performed to determine the impact of mixing and vapor phase cracking. Significance has been tested using a one tailed comparison of means in most cases, with two tailed comparisons being used where applicable. Statistical significance is reported through the use of p values; these values represent the probability that any differences between the data sets can be attributed to random error.

3.2.4   Analysis

In order to determine the extent of cracking reactions, density and viscosity of the product oil were analyzed using an Anton Paar SVM 3000 Viscometer. All viscosity measurements were conducted at a temperature of 60 °C, as the heaviest of the collected oil samples had a sufficient viscosity to prevent accurate determination at lower temperatures. In addition, the relative molecular weights of the product liquid were measured with a Waters Breeze GPC-HPLC (Gel Permeation Chromatography-High Performance Liquid Chromatography) instrument (1525 binary pump, Waters Styrylgel HR1 column at a temperature of 40 °C; UV detector at 270 nm). The GPC-HPLC was calibrated with linear polystyrene standards, and utilized THF as an eluent at a flow rate of 1 mL/min. The composition of gaseous components was found using two Varian CP 4900 3-Column Micro Gas Chromatographs.

3.3   Results and Discussion

The products of the Fluid Coking process were solid petroleum coke, liquid product oil, and non-condensable gases. A typical composition of non-condensable gases is shown in Table 3-3. The major components of these gases were found to be hydrogen and C1-C4 hydrocarbons, which comprise nearly 97 mol% of the stream. Limited amounts of carbon monoxide, carbon dioxide, and hydrogen sulphide were present due to the small amounts of oxygen and sulphur in the sample bitumen.

Table 3-3 - Typical composition of product gas

Gas Component	Mole Fraction (%)
Hydrogen	73.8
Hydrogen Sulphide	2.0
Methane	7.0
Carbon Monoxide	0.6
Carbon Dioxide	0.6
Ethylene	2.6
Ethane	3.2
Propane	7.5
Butane	2.8

It was observed that agglomerates were present with a diameter ranging from 355 µm to over 9500 µm (Figure 3-4). Small agglomerates were present in abundance while large agglomerates were far less common. Agglomerates larger than 9500 µm were only found when the mixer was not employed. However, larger agglomerates introduce heat and mass transfer limitations within the reactor, which result in slower reaction rates, longer diffusion pathways for product vapors, and a higher probability of coke-forming side reactions (Ali et al., 2010; Gray et al., 2001).

Figure 3-4 - Agglomerates formed during coking process

3.3.1   Short Vapor Phase Residence Time

Applied bed mixing was found to have a significant impact on agglomerate distributions. Figure 3-5 indicates that increased bed mixing resulted in drastic reductions in the cumulative mass of agglomerates above 600 µm. It can also be shown that the variability of the total mass of agglomerates was higher for the poorly mixed case (0 RPM), while applied bed mixing resulted in higher reproducibility of agglomerate distributions (100 RPM). It appears as though temperature fluctuations were responsible for

discrepancies between replicate experiments. Temperature fluctuations of 6 °C were observed in the reactor and are believed to result in fluctuations in the coking reaction rate (Toosi, McCaffrey, & de Klerk, 2013). An investigation by Weber (2009) indicated that reduced temperatures result in increased agglomerate stability due to the liquid binder experiencing slow reaction rates, thus giving agglomerates an increased likelihood of incorporating surrounding particles into the agglomerate and maintaining stability. Higher temperatures experienced faster reactions rates and vapor evolution, leading to agglomerate destabilization (Weber, 2009). It is inferred that, with the poorly mixed conditions at 0 RPM, any agglomerates that formed would be susceptible to temperature fluctuations, and therefore fluctuations in agglomerate stability. This would lead to variability in agglomerate distributions, as have been seen in this case. However, the use of the mixer provided increased reproducibility by destroying both stable and unstable agglomerates, thus dampening the effects of temperature fluctuations.
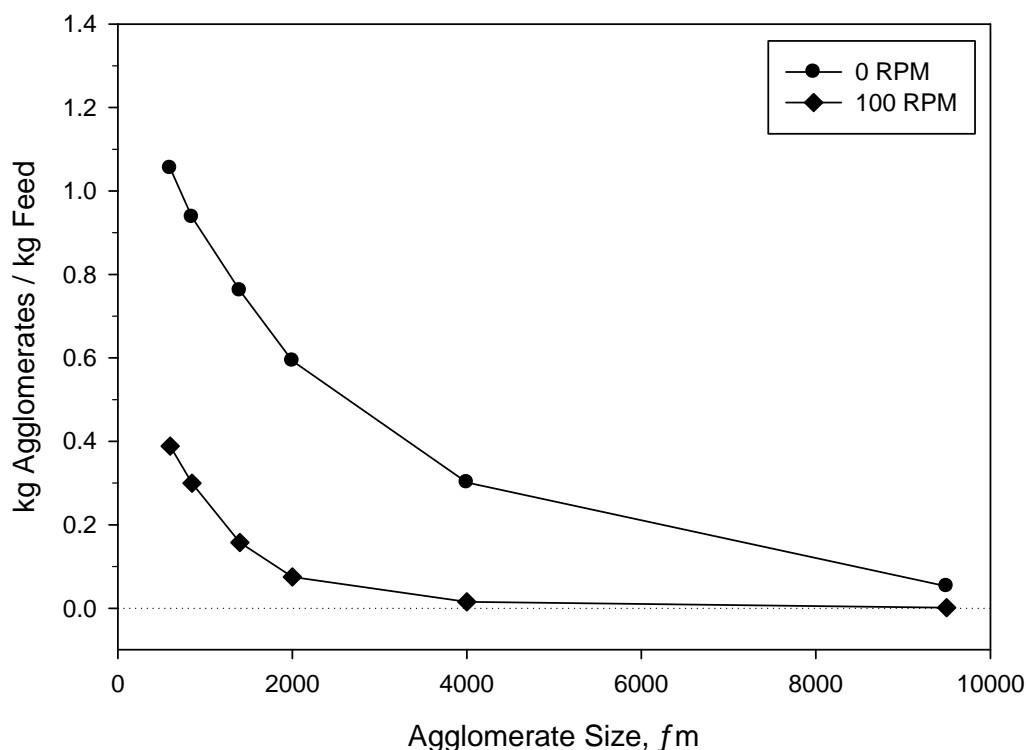

Figure 3-5 - Effect of agitation on cumulative agglomerate distributions at short vapor residence times (reactor temperature = 530 °C; vapor phase residence time = 5.3 s; error bars represent one standard deviation)

The reduction in total agglomerate mass can be attributed to the grinding aspect of the mixer blade incorporated in the reactor. The mixer blade impacts large agglomerates and grinds them against the distributor plate, fracturing them and redistributing the liquid among the surface of multiple fragments which may then form smaller agglomerates. These smaller agglomerates are expected to experience reduced mass and heat transfer limitations over the larger agglomerates, allowing coking reactions to occur at a faster rate than previously experienced (Ali et al., 2010; Weber, 2009). The fluidization gas also provides shear forces which help to fragment larger agglomerates and distribute them among the bed, forming small agglomerates (Weber et al., 2008).

It has been determined that there was a 2 wt% decrease in coke yields as mixing levels were increased. Coke yields dropped from 27 wt% at the poorly mixed condition to 25 wt% at the well-mixed condition. In addition, a positive correlation has been found between the cumulative mass of agglomerates and coke yield. This indicates that, at the well-mixed conditions at 100 RPM, agglomerate breakage and subsequent liquids dispersion was responsible for the decrease in coke yield. As agglomerates were broken down and liquid was dispersed quickly, the reduction in mass and heat transfer limitations reduced the likelihood of coke forming side reactions. The probability that the differences between the data sets at 0 and 100 RPM can be attributed to random error is only 11 %.

At short vapor residence times, the liquid yield increased with the increase in agitator speed, and these results are consistent with the results obtained in the Mechanically Fluidized Reactor (Chapter 2). Liquid yields increased from 65.5 to 67.5 wt% with applied bed mixing. A correlation between cumulative agglomerate distributions and increased liquid yields indicated that agglomerate destruction and liquid dispersion was responsible for the increase in liquid yield. Gas yields of approximately 7.5 wt% were obtained in the FCR. Gas yields differed by a mere 0.3 wt% between the poorly mixed and well-mixed cases, as the liquid released from agglomerates did not spend sufficient time in the vapor phase to crack to gas. From a statistical standpoint, gas yields are not affected at short residence times, as was seen in the MFR.

Increased agitator speeds were investigated on this reactor, however, the design of the mixer blade did not allow for successful experimentation at speeds approaching 200 RPM. The slight penetration of the nozzle tip into the reactor bed did not allow for the mixer blade to scrape the wall. For this reactor configuration, the mixer blade width was reduced in order to prevent nozzle damage. This resulted in a 5 mm annulus between the mixer blade and the reactor wall in which fluidization gas was the dominant mechanism of agglomerate breakage. At agitator speeds of 200 RPM, solids were pushed towards the wall by the mixer blade and did not have sufficient time to be dispersed by fluidization gas in between successive passes of the mixer blade. This resulted in wet solids being packed against the reactor wall, which eventually led to complete coking of the solids and drastically reduced liquid yields. In order to achieve successful bed mixing at such high speeds, the agitation system requires a complete redesign in order to mix the bed while not interfering with the injection nozzle.

Product oil dynamic viscosity and average molecular weight measurements have been conducted in order to determine the extent of thermal cracking reactions. Oil viscosity was found to decrease from 71 to 41 cP with applied bed mixing. Average molecular weight reduced from 365 to 352 g/mol. Combined with agglomerate breakage and the increase in liquid yield that has been established, these results indicate that the liquid trapped in the agglomerates was more reactive once it had been released and dispersed across the bed. This more reactive liquid underwent cracking reactions faster than the bulk of the liquid released during normal coking, leading to an increased yield of lower viscosity, lower-molecular weight liquid.

3.3.2   Long Vapor Phase Residence Time

Figure 3-6 demonstrates the cumulative mass of agglomerates larger than 600 μm at various residence times and agitator speeds. It is evident that there was essentially no impact of vapor residence time on agglomerate distributions at both the poorly and well-mixed cases. This was to be expected, as the vapor residence time facilitates vapor phase cracking reactions, which were not anticipated to generate significant quantities of coke or impact the agglomerate distribution.

Figure 3-6 - Effect of mixing on agglomerate distribution at long vapor residence time (temperature = 530 °C; vapor phase residence time = 13.0 s)

Figure 3-7 - Effect of mixing on coke yield at long vapor residence time (temperature = 530 °C; vapor phase residence time = 13.0 s; p = 0.39)

Figure 3-7 indicates that coke yield was not significantly impacted by vapor phase residence time. This is to be expected, as the increased vapor residence time impacts the cracking of vapor phase products into gas, which should have no discernible impact on agglomeration or the quantity of coke produced in the bed. Increased bed mixing was found to reduce the coke yield at both vapor residence times. Based on the known relation between the cumulative mass of agglomerates and coke yield, this reduction in coke yield can be attributed to agglomerate fracture and redistribution of the trapped liquid.

From Figure 3-8 it was found that mixing reduced liquid yields at prolonged vapor residence times. The long residence time employed in this reactor configuration resulted in vapor phase cracking of both the bulk of the liquid that was produced during normal coking reactions, as well as the more reactive liquid released from agglomerates. Liquid yields without a mixer were approximately 65 wt%, dropping to 63 % when mixing was applied. Overall, liquid yields were lower at prolonged residence times than, as is expected.

Figure 3-8 - Effect of mixing on liquid yield at long vapor residence time
(temperature = 530 °C; vapor phase residence time = 13.0 s; p = 0.05)
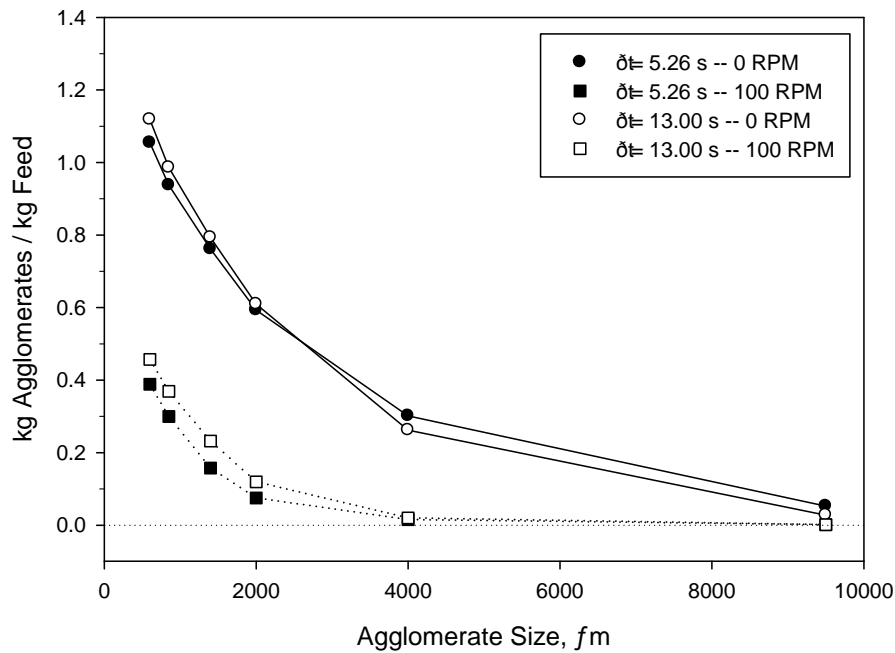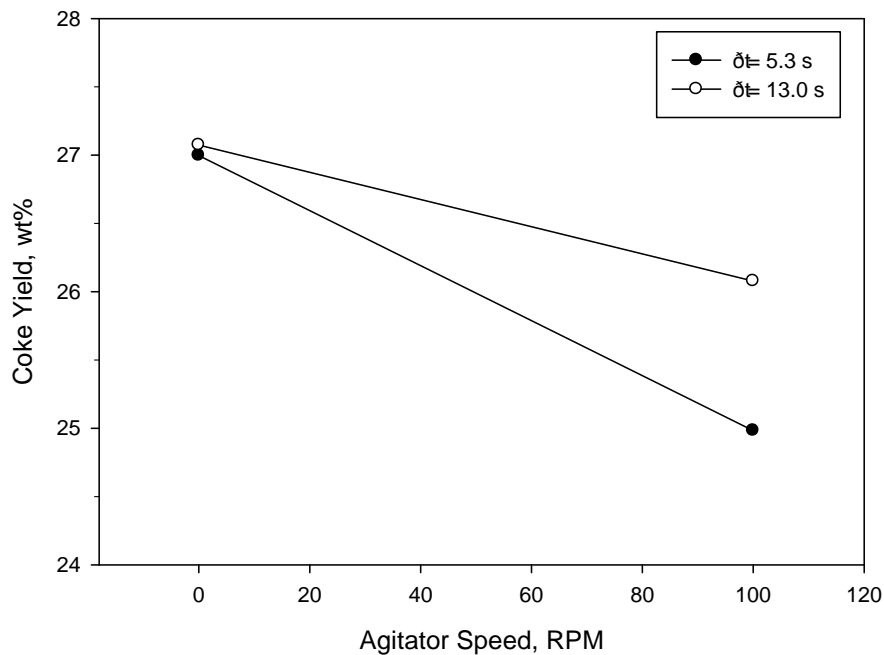
Figure 3-9 - Effect of mixing on gas yield at long vapor residence time (temperature = 530 °C; vapor phase residence time = 13.0 s; p = 0.01)

Figure 3-9 illustrates the effects of bed mixing on gas yields at prolonged vapor phase residence times. Increased levels of mixing have been found to drastically increase the gas yield. However, this was only found at prolonged residence times. At poorly mixed conditions at 0 RPM the average gas yield was 8.5 wt%, which increased by 2.7 wt% when agitation was applied. At prolonged residence times vapor phase cracking reactions were allowed to continue in the freeboard extensions, which acted to convert vapor products into noncondensable gas. There is a statistically significant increase in gas yield due to increased agitator speed. In addition, it was observed that gas yields were, overall, higher at prolonged residence times than short residence times. This occurred at poorly mixed and well-mixed conditions. The increase can be attributed to the vapor cracking reactions converting both bulk liquid produced during coking as well as liquid released from agglomerates.
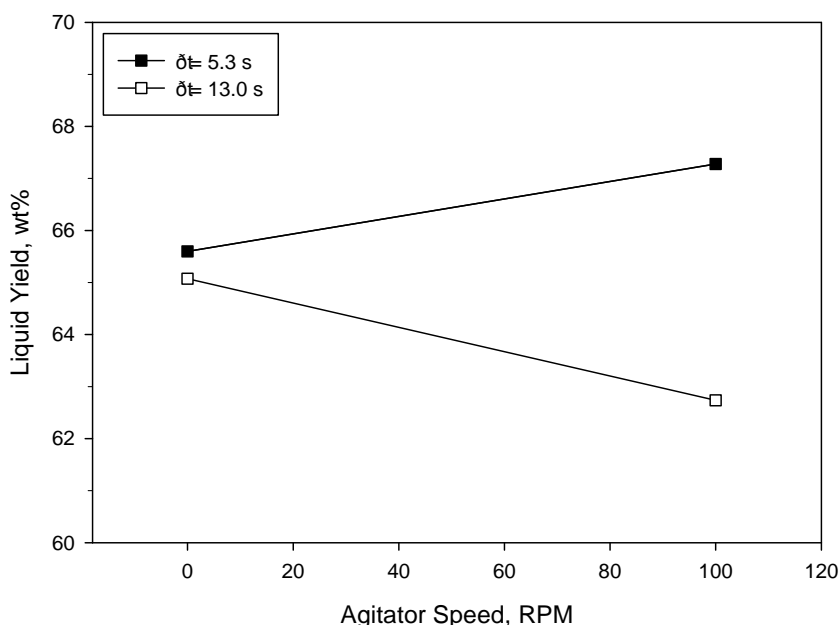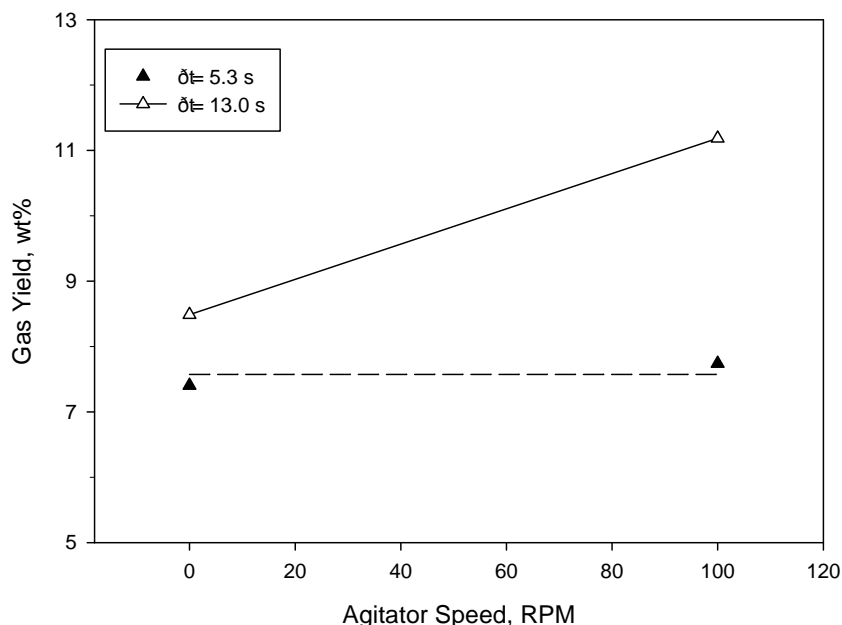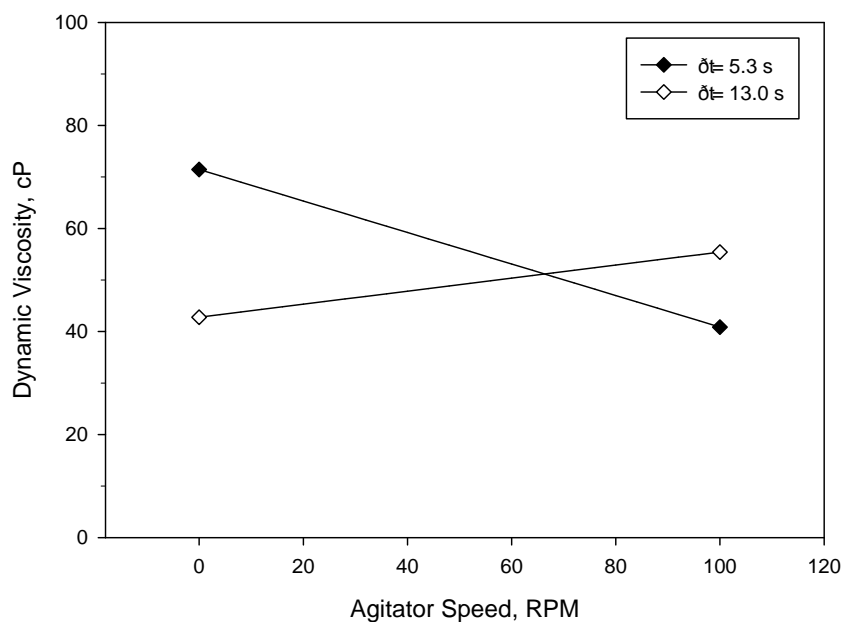
Figure 3-10 - Effect of mixing on viscosity at long vapor residence time (temperature = 530 °C; vapor phase residence time = 13.0 s; p = 0.02)
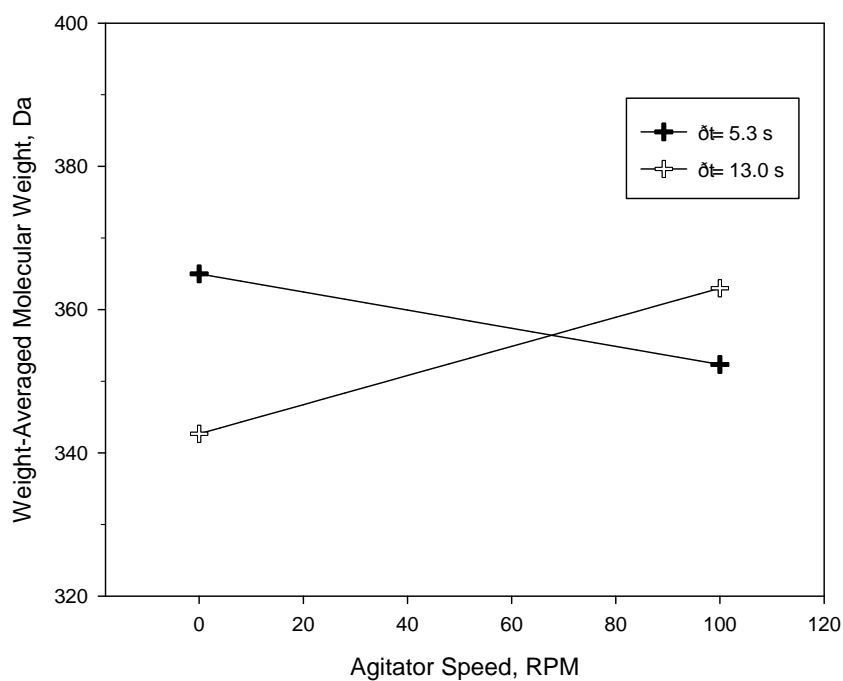

Figure 3-11 - Effect of mixing on molecular weight at long vapor residence time (temperature = 530 °C; vapor phase residence time = 13.0 s; p = 0.04)

As depicted in Figure 3-10, product oil viscosity increased with applied bed mixing at long vapor residence times. Comparison of means between these data sets indicated a statistically significant difference in viscosity due to the high reproducibility of the analysis. At longer residence times, agglomerate fracture and release of liquid coupled with prolonged vapor cracking reactions resulted in a net decrease in liquid yields. The result of these vapor phase cracking reactions was a concentration of more viscous products in the vapor phase that were unable to fully react to condensable gas, leading to an overall increase in liquid product viscosity.

Figure 3-11 highlights the impact of mixing on molecular weight at prolonged vapor residence time. At short residence times, applied bed mixing was found to reduce molecular weight as the liquid released from agglomerates was more reactive than the bulk of the liquid produced during coking. However, at prolonged vapor residence times there was a reduction in liquid yield and subsequent increase in gas yields, consistent with vapors being cracked to non-condensable gas. Given the molecular weight increase at long residence times, it appears as though the lighter, more reactive compounds in the vapor phase crack to gas while heavier, high molecular weight compounds are unable to react to the same extent, and are inversely concentrated in the liquid product.

3.3.3   Statistical Significance

Table 3-4 highlights the statistical significance of the impact of residence time on product yields and quality. It was found that prolonged vapor phase residence time had a significant impact on liquid and gas yields at both the poorly-mixed and well-mixed cases. As vapor residence time was increased there was a 92 % probability of a reduction in liquid yields with a corresponding increase in gas yields. In terms of product quality, prolonged residence time decreased viscosity and average molecular weight at the poorly-mixed case. These results had a 2 % probability of being attributed to error. At the well-mixed case, viscosity and molecular weight increased with prolonged residence time, with a probability of greater than 87 %. No significant impact of vapor residence time on coke yield has been found.

Table 3-4 - Effect of residence time

	Impact of prolonged residence time	p-value
0 RPM		
Liquid Yield	Decrease	0.08
Gas Yield	Increase	0.08
Viscosity	Decrease	0.01
Molecular Weight	Decrease	0.02
Coke Yield	Two-tailed	0.69
100 RPM		
Liquid Yield	Decrease	0.02
Gas Yield	Increase	0.00
Viscosity	Increase	0.01
Molecular Weight	Increase	0.13
Coke Yield	Two-tailed	0.41

Table 3-5 - Effect of mixing

	Impact of increased mixing	p-value
Short Residence Time		
Liquid Yield	Increase	0.16
Gas Yield	Increase	0.40
Viscosity	Decrease	0.01
Molecular Weight	Decrease	0.02
Long Residence Time		
Liquid Yield	Decrease	0.05
Gas Yield	Increase	0.01
Viscosity	Increase	0.02
Molecular Weight	Increase	0.04
Average of Residence Times		
Coke Yield	Decrease	0.09

Table 3-5 illustrates the statistical significance of mixing effects at short and long residence times. At short residence times, increasing bed mixing had an 84 % probability of increasing liquid yields. Given the agglomerate distributions found within this reactor and associated scatter during replicate experiments, the lower than expected significance for liquid yields could be improved by upgrading the temperature control on the reactor, which is likely the cause of the variability in agglomerate formation under the poorly mixed conditions. It is anticipated that improved temperature control would lead to

higher reproducibility in agglomerate distributions under poorly mixed conditions, which would result in more accurate quantification of the associated liquid yields. It has been found that mixing did not impact gas yields at short vapor residence time. It has also been determined that there was a minimum of 98 % probability that there were significant reductions in product oil viscosity and molecular weight with applied bed mixing.

This reactor configuration provided improved reproducibility at prolonged residence times (Table 35). The liquid yield decrease and subsequent gas yield increase had greater than 95 % probability of being attributed to mixing. At the same time, viscosity and molecular weights for the liquid samples appeared to increase; both of which had a greater than 96 % probability of being attributed to mixing. As it has been previously established that vapor residence time does not impact coke yields, these data have been merged to gain a more accurate determination of the impacts of mechanical agitation. It can be concluded that applied bed mixing had a 91 % probability of reducing coke yields using this reactor and mixer configuration.

3.3.4 Comparison Between Fluid Coking Reactor and Mechanically Fluidized Reactor

Figure 3-12 highlights the comparisons between the cumulative agglomerate distributions found on the Fluid Coking Reactor and Mechanically Fluidized Reactor (see Chapter 2). Comparing the poorly mixed conditions for both the FCR (0 RPM) and MFR (20 RPM) indicates the differences in mixer design and use of fluidization in the FCR. Figure 3-18 indicates that both reactors yielded comparable agglomerates larger than 4000 µm. However, agglomerates larger than 9500 µm were not as abundant in the FCR, likely due to the agitation provided by the fluidization gas. An investigation by Weber (2009) determined that large agglomerates are less stable than their smaller counterparts, and indicated that 10000 µm agglomerates fragment up to 150 % more than 5000 µm agglomerates. It was concluded that the instability of large agglomerates leads to extensive fracturing into smaller, wet fragments which continue to contact bed coke to produce small agglomerates (Weber, 2009). A study by Parveen et al. (2012) also indicates that gas bubbles contribute significantly to agglomerate breakage, in particular near the bed surface when gas bubbles explode (Parveen, Josset, Briens, & Berruti,

2012) These results are consistent with the FCR results, as there were fewer 9500+ μm agglomerates than in the MFR, due to fluidization bubbles contributing shear forces which selectively fragmented large agglomerates. These large agglomerates survived the MFR at the 20 RPM condition as there was no fluidization gas to contribute shear forces. It has also been found that there are increased levels of small agglomerates in the FCR consistent with large agglomerates fracturing and contacting individual bed coke particles to reform small agglomerates
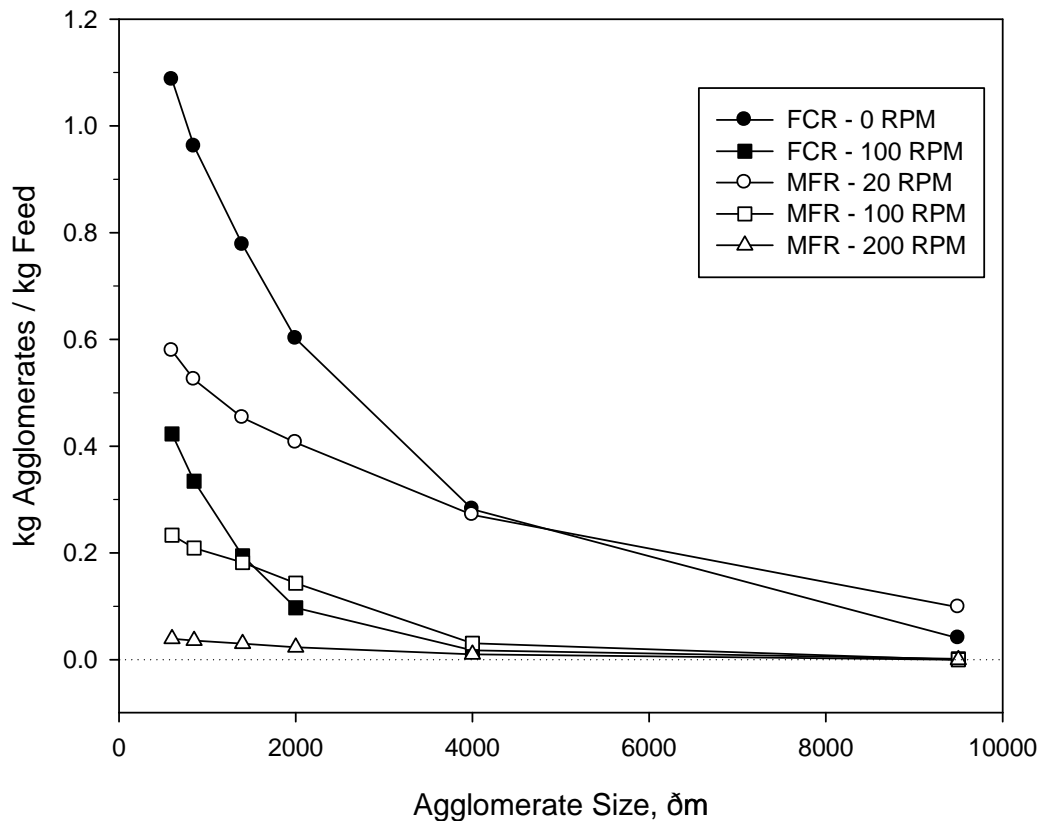

Figure 3-12 - Comparison of cumulative agglomerate distributions for FCR and MFR under varying agitator speeds

A comparison of both reactors at 100 RPM shows subtle differences as (Figure 3-12). Both reactors essentially eliminated 4000+ μm agglomerates at these mixer speeds through extensive agglomerate fragmentation. However, agglomerates smaller than 1400 μm were significantly more abundant in the FCR than the MFR, as the mixer did not fully scrape the wall and allowed smaller agglomerates to bypass the mixer blade and survive. A comparison cannot be made at 200 RPM due to the FCR inoperability under these conditions. It is anticipated that, with a redesign of the FCR mixer to approach that of the MFR, there would be comparable agglomerate distributions between the reactors independent of mixing levels (Appendix C).

Figure 3-12 shows that the FCR operated at 100 RPM had a cumulative mass of agglomerates that lies between MFR at 20 and 100 RPM. The coke yield for the FCR at 100 RPM was also found to lie between the coke yields of the MFR at 20 and 100 RPM, due to the nature of agglomeration impacting solid yields. From a statistical standpoint, the FCR coke yield at 100 RPM did not match the MFR at the same mixer speed, nor at the 20 RPM condition. This result highlights the fact that small differences in agglomerate distributions have corresponding impacts in coke yields, which would naturally influence the yield and quality of liquid produced. The differences in agglomerate distributions for seemingly comparable conditions have been found to have significant impacts on yields, leading to difficulties in directly comparing the reactors.

Figure 3-13 demonstrates the positive correlation between coke yield and mass of agglomerates larger than 600 μm. Both the FCR and MFR results showed a positive correlation between agglomerates and coke yield, indicating that coke yield was reduced as agglomerates were destroyed and dispersed their liquid across the reactor bed. Figure 3-14 demonstrates the negative correlation between liquid yields at short residence time and the cumulative mass of agglomerates. It was determined that agglomerate breakage and liquid dispersion led to an initial increase in liquid yields for both reactors. This correlation is less pronounced at prolonged vapor phase residence due to the simultaneous impact of agglomerate breakage and vapor cracking reactions on liquid yields.
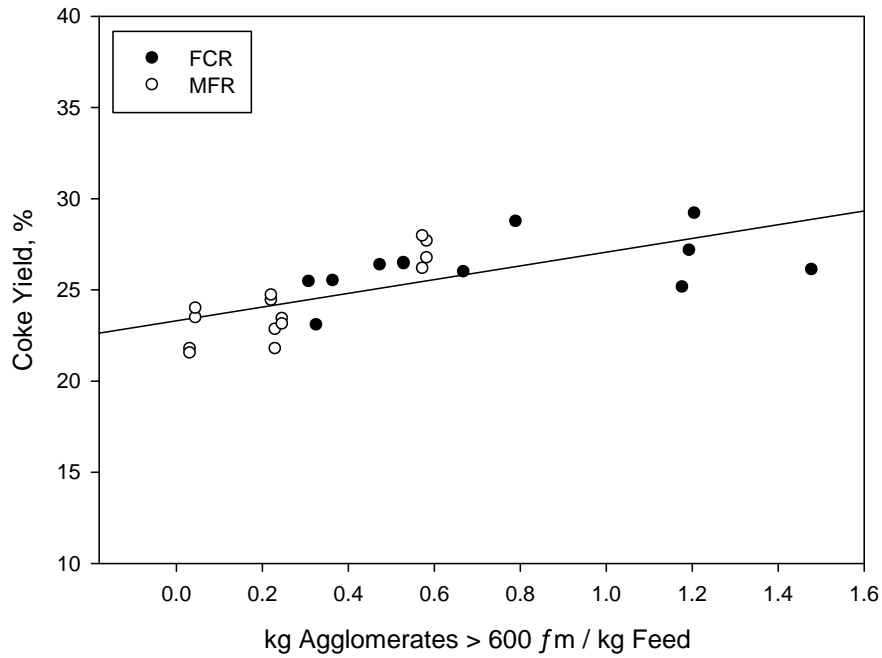
Figure 3-13 - Relation between coke yield and cumulative mass of agglomerates for FCR and MFR
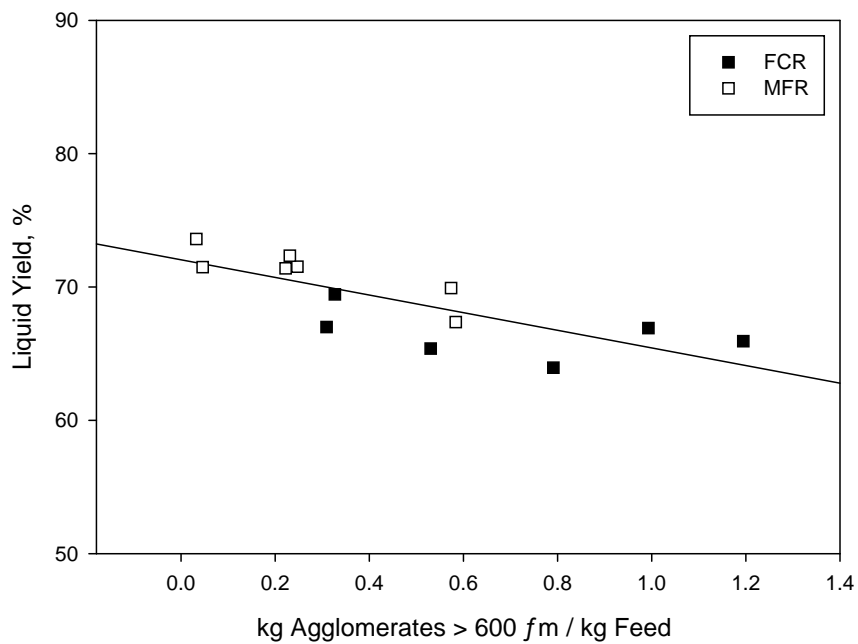

Figure 3-14 - Relation between liquid yield and cumulative mass of agglomerates for FCR and MFR

A direct comparison between the coke, liquid, and gas yields cannot be made at present due to the subtle differences between each reactor. It is likely that differences in injection may lead to differing sizes of initial agglomerates. The MFR injection does not disperse feed liquid effectively, which may lead to increased agglomerate (House et al., 2008). The FCR nozzle provides a more effective spray, which would theoretically lead to a decrease in initial agglomerate size. The fluidization within the FCR also leads to an increased likelihood of the destruction of large agglomerates. In addition, the known differences in mixer design have been shown to directly impact agglomerate distributions between the reactors. Given the differences in the cumulative mass of agglomerates found at 100 RPM in both reactors, it is evident that differences in mixer design do impact agglomerate destruction with a corresponding impact on coke yields. The relationship between agglomerates and liquid yield therefore poses a challenge in comparing the liquid yields in the reactors, while slight differences in vapor phase residence time also impact the conversion of liquids into gas. As such, no direct comparison can be made between coke, liquid, or gas yields at this time.

3.3.5 Impact of Atomization Degradation

Reductions in atomization gas-liquid ratio (or GLR) were carried out for two specific reasons. Mainly, it is beneficial to minimize the gas flowrates in order to minimize atomization gas cost while still maintaining reactor operability. Reactor response to poor atomization of liquids and the minimum successful GLR can be determined through experimentation under reduced GLR with applied agitation. In addition, it is necessary to determine whether the agitation system is capable of compensating for poor liquids injection characteristics, and the corresponding impact on the yield and quality of the liquid product. This was accomplished by reducing the atomization gas flowrate, and hence the GLR, with applied bed mixing.

The injection nozzle used in this reactor configuration is typically operated at a gas-liquid ratio of 105 wt%. This GLR provides very effective atomization of liquid droplets, as demonstrated in open spray tests. A poor injection GLR of 2 wt% was selected, as well as an intermediate GLR of 80 wt%. At a gas-liquid ratio of 105 wt%, the nozzle provided an even spray with fine bitumen droplets being created. As the GLR

was dropped, deterioration of the spray quality began. In the range 100-80 GLR, there was insufficient gas flow to fully atomize the bitumen. Bitumen droplets began to form on the bottom of the nozzle tip and the spray became interrupted by large droplets being carried intermittently into the spray region. As GLR was reduced further, the gas flow was insufficient to atomize any of the injected liquid, resulting in bitumen pouring from the nozzle tip towards the reactor distributor.

When agitation was not incorporated into the reactor, poor atomization conditions and bitumen dripping resulted in severe operational problems. Without proper atomization, the injected bitumen experienced poor penetration resulting in agglomerate formations localized on the nozzle tip. If the fluidization and atomization gases did not immediately remove the initial agglomerate from the tip, fresh oil was laid down on top of it, resulting in further contact with bed solids and further growth of the agglomerate. Over time, fresh oil was continuously laid down as a large agglomerate around the nozzle tip which began to further degrade atomization quality and interfere with oil injection. In some instances the agglomerate continued to grow out and away from the tip while allowing for injection to continue unimpeded. However, more often than not, poor atomization resulted in agglomerate formations which completely blocked injection and forced the reactor into premature shutdown. The problematic injection resulted in drastically reduced liquid yields due to feed being trapped in large agglomerate formations.

When agitation was applied to the bed, it was found that injection degradation has no impact on reactor operability. The mixer was fully capable of compensating for poor injection that would have otherwise taken the reactor offline. With applied agitation, it was found that there was no significant difference in liquid yields and product quality when comparing high and low GLR injections.

As the nozzle tip extends beyond the nozzle jacket in order to promote external mixing, the tip was susceptible to damage over the course of multiple injections. With near perfect alignment within the center of the nozzle, the atomization gases were capable of surrounding the entire of the nozzle tip and providing an even spray distribution (at 105 wt% GLR). However, any damage to the nozzle tip led to a misalignment, which

disrupted the normal flow pattern at the tip. In multiple instances, the nozzle tip was deflected in one direction, resulting in a loss of proper atomization on that side of the nozzle. This has been observed to cause complete disruption of the atomization flow, resulting in bitumen dripping from the nozzle tip and into the bed. Under poorly mixed conditions at 0 RPM, nozzle damage resulted in agglomerate formations comparable to reduced GLR injection, leading to similar reactor shutdown. However, it has been found that well-mixed conditions at 100 RPM resulted in liquid yields comparable to high GLR injection, further reinforcing the advantage of applied bed mixing to reduce agglomerate formations and redistribute liquid across the reactor bed.

3.3.6 Impact of Temperature

At present, the Fluid Coking Reactor is not capable of sustained operation at temperatures below 530 °C. The reactor could not be reliably operated at a temperature of 510 °C. Heat and mass transfer limitations within the agglomerates coupled with the poorly-mixed conditions that were tested led to an increase in the required minimum fluidization velocity, the consequence being catastrophic defluidization or "bogging" (Briens et al., 2003). This loss of fluidization led to complete reactor inoperability and solidification of the entirety of the reactor bed.

In addition, the reactor frequently experienced temperature fluctuations of ± 8 °C which were believed to result in fluctuations in the cracking reaction rate. Variability in reaction rates would result in variability in agglomerate distributions for the poorly mixed case only (as has been observed), as the agitator was fully capable of compensating for severe agglomeration. The results obtained at a reduced temperature and fluctuations that have been experienced indicate that improved temperature control is necessary for this reactor in order to attain increased reproducibility in coke and liquid yields. The MFR (Chapter 2) used a more effective agitator and induction heating to provide improved temperature control.

3.4 Conclusions

The impact of applied bed agitation on Fluid Coking€ agglomerate distributions and yields has been successfully investigated in a pilot-scale fluidized bed reactor. Separate vapor phase residence times have been employed to determine the impacts of vapor phase cracking on liquid and gas yields. In addition, the impact of bed mixing and vapor phase cracking on liquid quality has been confirmed using this reactor configuration.

It has been found that bed mixing was responsible for agglomerate breakage and control over the agglomerate distribution within the reactor. In addition, agglomerate breakage has been found to reduce coke yields due to the release and dispersion of trapped liquid feed. Agglomeration within cokers results in the entrapment of feed bitumen, ultimately leading to reduced liquid yields due to the mass and heat transfer limitations of larger wet agglomerates. Agglomerate breakage and subsequent liquid dispersion results in increased yields of low-viscosity, low-molecular weight liquid at short vapor residence times. However, the liquid released from agglomerates was more reactive and continued to crack to gas at prolonged vapor phase residence times, resulting in a concentration of higher-viscosity, higher-molecular weight compounds in the liquid phase. This study highlights the importance of quick agglomerate breakage and feed dispersion in Fluid Cokers by relating agglomerate destruction to the quantity and quality of liquid product that can be attained. It has also been determined that the mixer system employed on this reactor was fully capable of compensating for poor liquid injection. Injection degradation through the use of reduced gas-liquid ratios and nozzle damage indicate that the mixer system allows the reactor to maintain operability under conditions that lead to severe agglomeration and complete injection blockage. In addition, drastic agglomeration experienced at reduced temperatures indicate that the reactor requires improved temperature control in order to attain increased reproducibility of agglomerate distributions and, subsequently, coke and liquid yields.

3.5 References

Ali, M., Courtney, M., Boddez, L., & Gray, M. (2010). Coke Yield and Heat Transfer in Reaction of Liquid‐Solid Agglomerates of Athabasca Vacuum Residue. The Canadian Journal of Chemical Engineering, 88(1), 548.

Aminu, M. O., Elliott, J. A. W., McCaffrey, W. C., & Gray, M. R. (2004). Fluid Properties at Coking Process Conditions. Industrial & Engineering Chemistry Research, 43(12), 2929‐2935.

Ariyapadi, S. (2004). Interaction Between Horizontal Gas‐Liquid Jets and Gas‐Solid Fluidized Beds. The University of Western Ontario.

Ariyapadi, S., Holdsworth, D. W., Norley, C. J. D., Berruti, F., & Briens, C. (2003). Digital X-ray Imaging Technique to Study the Horizontal Injection of Gas‐Liquid Jets into Fluidized Beds. International Journal of Chemical Reactor Engineering, 1.

Briens, C., McDougall, S., & Chan, E. (2003). On-line detection of bed fluidity in a fluidized bed coker. Powder Technology, 138(2‐3), 160‐168.

Darabi, P., Pougatch, K., Salcudean, M., & Grecov, D. (2010). Agglomeration of Bitumen‐Coated Coke Particles in Fluid Cokers. International Journal of Chemical Reactor Engineering, 8.

Gray, M. R. (2002). Fundamentals of Bitumen Coking Processes Analogous to Granulations : A Critical Review. The Canadian Journal of Ch 80(June), 393‐401.

Gray, M. R., Le, T., McCaffrey, W. C., Berruti, F., Soundararajan, S., Chan, E., ƒ Thorne, C. (2001). Coupling of Mass Transfer and Reaction in Coking of Thin Films of an Athabasca Vacuum Residue. Industrial & Engineering Chemistry Research, 40, 3317‐3324.

Gray, M. R., Le, T., & Wu, X. A. (2007). Role of Pressure in Coking of Thin Films of Bitumen. The Canadian Journal of Chemical Engineering, 85(October), 773‐780.

Gray, M. R., McCaffrey, W. C., Huq, I., & Le, T. (2004). Kinetics of Cracking and Devolatilization during Coking of Athabasca Residues. Industrial & Engineering Chemistry Research, 43(18), 5438‐5445.

Gray, M. R., Zhang, Z., McCaffrey, W. C., Huq, I., Boddez, L., Xu, Z., & Elliott, J. a. W. (2003). Measurement of Adhesive Forces during Coking of Athabasca Vacuum Residue. Industrial & Engineering Chemistry Research, 42(15), 3549‐3554.

Hammond, D. G., Lampert, L. F., Mart, C., Massenzio, S. F., Phillips, G. E., Sellards, D. L., & Woerner, A. C. (2003). Review of Fluid Bed Coking Technologies (pp. 1‐8).

House, P. K., Briens, C. L., Berruti, F., & Chan, E. (2008). Effect of spray nozzle design on liquid‐solid contact in fluidized beds. Powder Technology, 186(1), 89‐98.

House, P. K., Saberian, M., Briens, C. L., Berruti, F., & Chan, E. (2004). Injection of a Liquid Spray into a Fluidized Bed: Particle‐Liquid Mixing and Impact on Fluid Coker Yields. Industrial & Engineering Chemistry Research, 43, 5663‐5669.

McCaffrey, D. S., Hammond, D. G., & Patel, V. R. (1998). Fluidised Bed Coking Utilising Bottom of the Barrel (pp. 1‐7).

Parveen, F., Josset, S., Briens, C., & Berruti, F. (2012). Effect of Size and Density on Agglomerate Breakage in a Fluidized Bed. Powder Technology, 231, 102‐111.

Pfeiffer, R. W., Borey, D. S., & Jahnig, C. E. (1959). Fluid Coking of Heavy Hydrocarbons. United States: United States Patent Office.

Salman, A. D., Fu, J., Gorham, D. ., & Hounslow, M. . (2003). Impact Breakage of Fertiliser Granules. Powder Technology, 130(1), 359‐366.

Sanchez, F. J., & Granovskiy, M. (2013). Application of radioactive particle tracking to indicate shed fouling in the stripper section of a fluid coker. The Canadian Journal of Chemical Engineering, 91(6), 1175‐1182.

Speight, J. G. (1998). Petroleum Chemistry and Refining. Washington: Taylor & Francis.

Teare, M., Cruickshank, R., Miller, S., Overland, S., & Marsh, R. (2014). Alberta‟s Energy Reserves 2013 and Supply/Demand Outlook 2014‐2023. Calgary.

Toosi, E., McCaffrey, W. C., & de Klerk, A. (2013). Copyrolysis of Oxygenate Containing Materials with Bitumen. Energy & Fuels, 27, 6433‐6439.

Weber, S., Briens, C., Berruti, F., Chan, E., & Gray, M. (2008). Effect of Agglomerate Properties on Agglomerate Stability in Fluidized Beds. Chemical Engineering Science, 63(17), 4245‐4256.

Weber, S. (2009). Agglomerate Stability in Fluidized Beds. The University of Western Ontario.

Chapter 4

4   Effects of Bed Mixing on Biomass Fast Pyrolysis

4.1   Introduction

Based on growing concerns of fossil fuels depletion and the environmental impact of burning conventional petroleum fuels for heat and electricity, there is an increasing interest in obtaining fuels from alternative resources. Biomass pyrolysis is an attractive waste-to-fuels process as it has the capability of converting agricultural and forestry wastes to useable fuel oil after upgrading and stabilization processes. As pyrolysis technology matures over the coming decades, it may have the capacity to become a competitive source of fuels and energy in the global market.

Pyrolysis is the thermochemical decomposition of biomass without oxygen. Biomass pyrolysis involves the fragmentation of high molecular weight lignocellulosic and extractive components into lower-molecular weight solid, liquid, and gaseous products (Mohan et al., 2006). It has been applied to an extensive variety of raw biomass (such as wood sawdust, straw and sugarcane), biomass components (cellulose, hemicellulose, and lignin), and waste compounds (such as sewage, construction waste wood, and tires). Applications of pyrolysis range from waste-to-energy production, pollution control, and landfill diversion (Dai et al., 2014; J. W. Kim et al., 2014; Martínez et al., 2013). In biomass pyrolysis, the high temperatures thermally crack the macromolecular structures of cellulose, hemicellulose, and lignin through primary pyrolysis reactions. These reactions produce non-condensable gases and low-molecular weight compounds which vaporize and exit the structure, leaving behind the solid char product (Bridgwater et al., 1999; Isahak et al., 2012; Neves et al., 2011). Pyrolysis yields and product composition are directly impacted by reactor temperature, heating rates, particle size, and reactor configuration, as well as the relative abundance of hemicellulose, cellulose, lignin and ash within the biomass feedstock. A comprehensive analysis of biomass pyrolysis is provided in Chapter 1.

An investigation into lignin pyrolysis in a fluidized bed reactor indicated severe particle bed mixing phenomenon that can occur with certain feedstock. It was found that, due to the low melting point of lignin, particles begin to heat up and melt even before injection is achieved. This study concluded that pneumatic injection of lignin into a fluidized bed as essentially impossible due to the plugging of injection lines (Nowakowski et al., 2010) The intermittent solid slug feeder system has been investigated in several recent studies, with feedstocks of sawdust, tucumã seeds, and meat and bone meal (Berruti, Ferrante, Berruti, & Briens, 2009; Berruti, Ferrante, Briens, & Berruti, 2012; Lira et al., 2013). This technology has been demonstrated to provide effective and consistent feeding rates without issue. Recent work by Gooty (2013) investigated Kraft lignin pyrolysis in a fluidized bed reactor using the intermittent feeder system. It was found that lignin particles that are successfully fed to the fluid bed experience immediate agglomeration with bed particles, resulting in severe blockages and catastrophic defluidization. Applied mechanical agitation demonstrated the capacity to destroy agglomerates, allowing for continuous pyrolysis to be carried out (Gooty, 2013). However, mechanical agitation for this system was an absolute necessity to facilitate prolonged injection, and not fully investigated to determine any subsequent impacts on the pyrolysis process.

The Fluid Coking process and fluidized bed pyrolysis share several similarities. Both processes employ a fluidized bed reactor at elevated temperatures to perform thermal cracking reactions in the absence of oxygen. The fluidized bed of heat carrier is used to provide effective mixing and heat transfer between the feedstock and bed material. In Fluid Coking, the feed liquid trapped in liquid-solid agglomerates undergoes primary cracking reactions which produce lower molecular weight components. These vapors diffuse out of the agglomerates, and may undergo intraparticle secondary reactions which increase the coke yield. In biomass pyrolysis, it is the solid particles themselves which undergo primary cracking reactions to produce vapor products. As with Fluid Coking, heat and mass transfer limitations result in intraparticle secondary reactions which reduce liquid yields and increase the production of solid char. Both processes employ short vapor residence times to limit vapor phase secondary reactions which convert valuable vapor products into non-condensable gas. Though biomass pyrolysis utilizes a solid feedstock, compared to liquids injection in Fluid Coking, the similarities between the

processes allow for biomass pyrolysis to be carried out in a Fluid Coking reactor to further develop an understanding of the impacts of applied bed mixing on the yield and quality of liquid products.

The objective of this study is to determine the limitations of a Fluid Coking Reactor in pyrolysis configuration. The liquid injection system is replaced with a pulsed solid injection system that has already been shown to provide better mixing of the feedstock powder with the bed particles than can be achieved with a standard screw feeder (Berruti, Ferrante, Briens, & Berruti, 2012). Specifically, the impact of applied particle bed mixing is to be determined in a non-agglomerating system, in contrast to previous studies on agglomerating systems. Quantification of the impact of bed mixing on the yield of bio-oil is confirmed at various operating conditions. In addition, analysis is carried out to determine the effect of mixing on the chemical composition of the produced bio-oil. Finally, this study demonstrates the influence of particle size on liquid yield production, while validating that smaller particles can be successfully injected using the existing feeder system.

4.2 Experimental

4.2.1 Materials

Birchwood was used as the feedstock for pyrolysis. Initial experimentation was carried out using a larger particle size of 500-600 …m. This particle size falls within the acceptable range of particle sizes for fast pyrolysis. Further experimentation was carried out using a reduced particle size of 125-250 …m. This particle size approaches the limitations of the feeding system, as smaller particles become more cohesive and hinder continuous feed rates. In addition, as particle size is reduced, the particle terminal velocity approaches that of the fluidization velocity in the reactor. It is expected that particles below 150 …m will be elutriated from the bed before reacting fully. This would result in particles accumulating on the reactor filter system, which would decrease the residence time of the evolved vapors and negatively influence the liquid yields observed during experimentation. Specifications for the birchwood feedstock are illustrated in Table 4-1.

Table 4-1 - Birchwood specifications

		Larger Particle Size	Smaller Particle Size
Particle Size Range	μm	500-600	150-225
Moisture Content	wt%	< 10	
Ash Content	wt%	~1.63	
Ultimate Elemental Analysis:			
Carbon	wt%	55.66	
Hydrogen	wt%	3.71	
Nitrogen	wt%	0.16	
Sulphur	wt%	0.00	
Oxygen (by difference)	wt%	40.47	

Nitrogen was utilized as fluidization, carrier, and pulse gas to obtain oxygen-free atmosphere for pyrolysis. The reactor bed was composed of silica sand having a particle density of 2650 kg/m³ and Sauter mean diameter of 150 …m. Total bed mass was held constant at 1.500 kg for each experiment.

4.2.2 Experimental Apparatus

Experimentation was carried out using a pilot-scale Fluid Coking Reactor (Figure 4-1). The pilot-scale system consists of a cylindrical fluidized bed reactor with an internal diameter of 0.076 m and total height of 0.594 m. The unit was operated at atmospheric pressure, with operating temperatures of 500 °C and 550 °C. The reactor was equipped with five Watlow mica electric band heaters. Fluidization gas was preheated using an Omega AHP-3742 in-line air heater. Reactor temperature control was provided by eight type K thermocouples, with accompanying Honeywell UDC200 Mini-Pro Digital controllers.

Figure 4-1 - Fluid Coking Reactor in pyrolysis configuration

Fluidizing gas was injected at the base of the reactor through a perforated design consisting of ten porous disks. The porous disks are arranged in a ring at the base of the mixer driveshaft (Figure 4-2) and have a pore size of 40 μ. The remaining gas entered through the solids feeding port, located 0.10 m above the distributor. The mixing system was mounted on the bottom of the reactor, with the driveshaft located in the center of the reactor flange (Figure 4-2). The mixer blade was driven by an electric variable speed motor, allowing for mechanical agitation speeds ranging from 0 to 200 RPM. The mixer blade orientation in the reactor was such that it scraped the wall of the reactor and drew solids into the center of the bed.

Figure 4-2 - Fluid Coking Reactor mixer assembly

4.2.3   Experimental Procedure

When operating in pyrolysis configuration, the fluid coking reactor utilized an intermittent solid slug feeder system (Berruti et al., 2012). A solids storage silo was fitted to the top of the reactor and contained a mixer system to prevent solids bridging, which results in undesirable fluctuations in feedrate. The silo was equipped with a pressure regulator which maintained the silo pressure slightly above that of the reactor. This was incorporated to prevent the backflow of hot solids from the reactor, through the feeder system and into the silo. Directly under the silo was a pneumatically actuated pinch valve, controlled by a system of solenoid valves (Granzow Inc. 21EN) and a relay timer (IMO iSmart Relay). Nitrogen pulses were delivered to the feeding tube using pressurized 80 mL steel canisters controlled by solenoid valves and the relay timer. The relay timer opened the pinch valve for a short interval. During this time, a slug of biomass dropped through the pinch valve into the feeding tube, and the valve closed. As the slug entered the feeding tube, a nitrogen pulse propelled the biomass slug along the

tube and into the reactor. In addition, a continuous flow of nitrogen was supplied along the feeding tube to prevent solids backflow and ensure that all of the biomass entered the reactor. The feeder system is depicted in Figure 4-3.

Figure 4-3 - ICFAR intermittent solid slug feeder system[2]

As the biomass entered the reactor, the slug disintegrated and dispersed across the reactor bed. At the elevated temperatures in the reactor, biomass thermally degraded into vapor and gas products through primary cracking reactions. A solid char was deposited on the bed coke particles. As the vapor products travelled up the reactor, they continued to undergo secondary cracking reactions in the gas phase. The product vapors travelled up through the freeboard before exiting through a filter (Figure 4-4). The

---

[2] Reprinted from Journal of Analytical and Applied Pyrolysis, 94, Berruti, F. M., Ferrante, L., Briens, C. & Berruti, F., Pyrolysis of cohesive meat and bone meal in a bubbling fluidized bed with an intermittent solid slug feeder, 153-162, Copyright (2012), with permission from Elsevier.

Figure 4-4 - Pyrolysis process diagram

product line exiting the reactor was maintained at 200 °C using double pipe heat exchange with heated air. This temperature has been found sufficient to reduce secondary reactions, while eliminating backpressure issues caused by vapor product condensation.

Immediately after the reactor were two cyclonic condensers in series, immersed in an ice water bath (Figure 4-4). Heavy fractions of the oil were collected in the bottom of the condensers, while noncondensable gases and entrained mist continued downstream to an electrostatic precipitator. Within the ESP, a voltage of 15 kV was applied between the electrode and ESP wall, resulting in ionization of the gas around the electrode through corona discharge. The entrained mist entering the ESP was charged by the ionized gas, and the electric field around the electrode forced the charged mist to the wall. Mist condensed on the wall and drained to the bottom of the ESP for collection. The non-condensable gases continued through a cotton filter and were vented to atmosphere.

For this study, the impacts of applied fluid bed mixing were carried out under two separate temperatures with two separate particle sizes. Separate temperature and particle sizes were tested to ensure that the impacts of mixing, if any, were reproducible under various reactor operating conditions. For all cases, pyrolysis was performed on 0.300 kg of biomass, with a feed rate of 1 kg/h and a vapor residence time of 0.8 s. The experimental procedure was as follows:

1. Initial experimentation was carried out at 550 °C without the mixer to determine the baseline liquid yields. A particle size of 500-600 µm was used.

2. Experimentation was performed at 550 °C with the mixer blade held stationary in the path of the solids injection port. This was performed to determine if impaction of solids onto the blade resulted in improved dispersion of the injected biomass particles. A particle size of 500-600 µm was used.

3. Pyrolysis was then carried out at a temperature of 550 °C at 60 and 100 RPM to determine the impact of applied solids mixing. Pyrolysis was accomplished using a particle size of 500-600 µm.

4. Experimentation was then carried out at a reduced temperature of 500 °C using 500-600 µm biomass. A variety of mixing speeds were used to confirm the impact of applied bed mixing at this temperature.

5. A reduced particle size of 125-225 µm was used at a temperature of 550 °C with and without bed mixing.

Statistical analysis has been performed to determine the impact of mixing under each operating condition. Significance has been tested using a tailed comparison of means. Statistical significance is reported through the use of p-values; these values represent the probability that any differences between the data sets can be attributed to random error.

4.2.4   Analysis

Analysis was carried out to characterize the impact of increased particle mixing on the chemical composition of collected bio-oil samples. Bio-oil was analyzed for water content, as well as concentrations of levoglucosan, acetic acid, and hydroxypropanone, as these are typically the abundant products of cellulose and hemicellulose degradation. Water content was determined using a Mettler Toledo V20 Volumetric KF Titrator. Concentrations of levoglucosan, acetic acid, and hydroxypropanone were determined using a Shimadzu GC-2010 equipped with an A0C-20i+s Autosampler.

4.3   Results and Discussion

4.3.1   Liquid Yield

The pyrolysis process laid down biochar on the bed sand and produced a dark brown liquid bio-oil exhibiting slight phase separation. Initial experimentation with a stationary blade indicated that there was no increase in liquid yield as a result of particle impaction on the stationary blade. As such, these values for a stationary blade have been combined and reported as the poorly mixed case represented by 0 RPM. As mechanical agitation was applied to the bed, the reactor system produced liquid yields as shown in Figure 4-5. Initial experimentation at a temperature of 550 °C with 500-600 µm particles produced average liquid yields of 51.3 ± 3.0 wt%. Over the range 0-60 RPM, there was no

difference in liquid yield. Between 60 0 RPM, the slight increase in liquid yield does not represent a statistically significant change. It can be concluded that there was essentially no improvement in liquid yield to be gained through increased particle bed mixing beyond the already effective mixing achieved with the pulsed feeder, which propels the biomass particles into the central, well-agitated region of the fluidized bed.
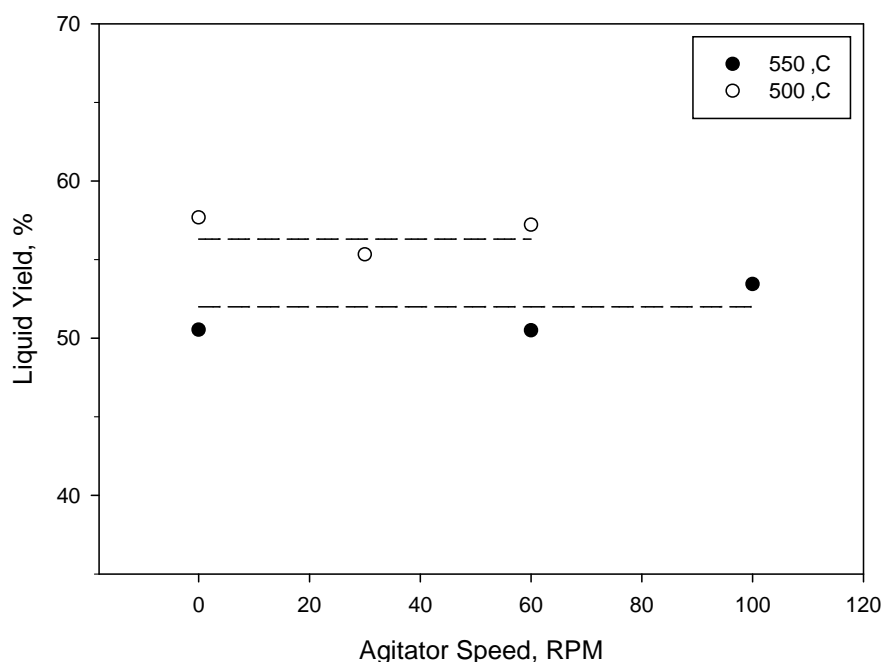

Figure 4-5 - Effect of temperature on birchwood fast pyrolysis (particle size = 500 0 600 µm; p_{550} = 0.39; p_{500} = 0.79)

Experimentation at 500 °C with 500 0 µm particles confirmed a negligible impact of feedstock bed mixing at separate operating conditions (Figure 4-5). Over the range of 0-60 RPM, there was minimal difference in liquid yield. Statistical analysis between the data sets indicated that liquid yields are not impacted by applied bed mixing. In addition, it was demonstrated that increased liquid yields could be attained at a temperature of 500 °C. Liquid yields were determined to be 57.0 ± 1.7 wt% at this temperature, a significant improvement over 550 °C.

Extensive research has been conducted into the effects of temperature on various feedstocks. Most biomass experiences maximum liquid yields within the range of 500-550 °C (Akhtar & Amin, 2012; Mohan et al., 2006). Vacuum pyrolysis of birchwood at a

temperature of 500°C has been studied recently, with liquid yields of 53.9 wt% being reported (Murwanashyaka et al., 2001). This was found to be slightly reduced over the above 500 °C results, however, the discrepancy can be attributed to the method of pyrolysis and the particle size used. Vacuum pyrolysis is known to produce reduced liquid yields compared to ablative and fluid bed pyrolyzers due to the slower heating rates used, as well as the larger particle sizes that are typical of this process (Bridgwater et al., 1999). Maximum liquid yields of birch pyrolysis oil have previously been found at a temperature of 500°C, which is in agreement with the above results (Drummond & Drummond, 1996).
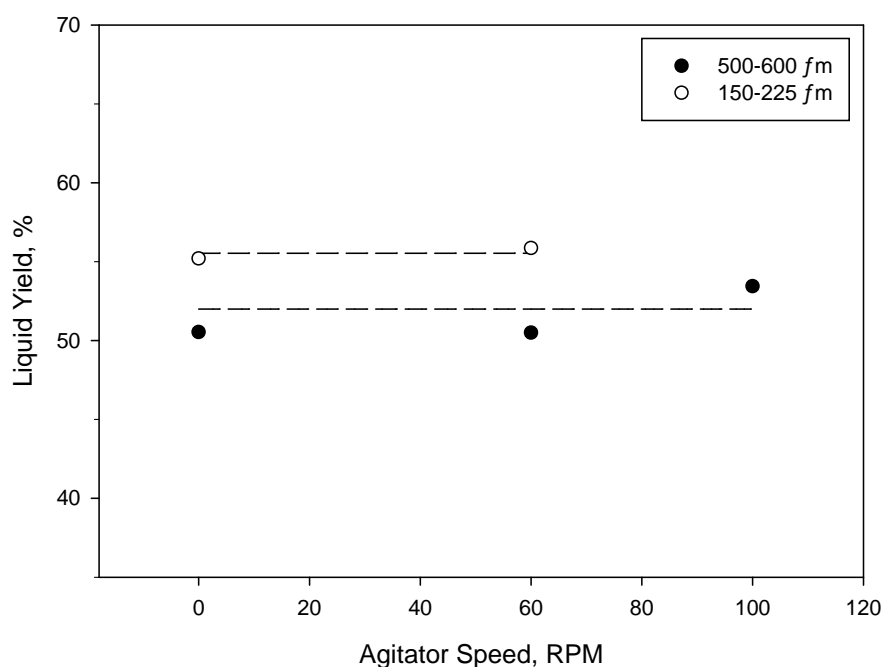

Figure 4-6 - Effect of biomass particle size on liquid yield (temperature = 550 °C)

Pyrolysis carried out using a temperature of 550 °C with a reduced particle size of 150-225 µm again indicated a negligible impact of additional feedstock mixing on liquid yields (Figure 4-6). These results confirmed that increased mixing between feedstock particles and bed sand provided no impact on liquid yields for the agglomerating system. While the reduction in particle size was found to have no discernible impact on the feed system operation, oil yields were slightly improved. Average liquid yields

using 150-225 µm particles were 55.4 ± 1.4 wt%, an increase of 4 wt% over the larger particle size. Comparison of means between the biomass particle sizes indicated a statistically significant improvement in liquid yields with the more finely ground feed.

The reduction in liquid yield experienced when biomass particle size was increased from 150-225 µm to 500-600 µm is attributed to internal heat and mass transfer limitations. Larger particles are more likely to experience temperature gradients and hinder diffusion of moisture and primary cracking products from inside the particle (Ishak et al., 2012; Neves et al., 2011). This has the effect of increasing the intraparticle secondary pyrolysis reactions, which have a tendency to produce higher yields of char and permanent gases through a variety of chemical reactions. The reduced particle size 225-150 µm experiences less intraparticle secondary reactions, leading to increased liquid yields over the 500-600 µm particles (Neves et al., 2011).

In addition, there is the possibility of the smaller particle size experiencing elutriation from the bed before reacting fully. Although the 150 µm particles have a terminal velocity greater than that of the bed fluidization velocity, it is possible that particle shrinkage or reduction in particle density could occur during pyrolysis, leading to the elutriation of reacting particles into the freeboard and onto the reactor wall (Davidsson & Pettersson, 2002). If this were to occur, it would lead to reduced vapor residence time of the primary pyrolysis products, serving to increase the liquid yield over what would be expected.

4.3.2   Composition

Slight phase separation was exhibited in the collected bio-oil samples. All samples were found to have a pH in the range of 2-3.5, with slightly more acidic oil being collected within the ESP. Analysis indicated an average water content of 8.9 ± 1.0 wt% of the bio-oil sample. Birchwood-derived pyrolysis oil with a reaction water content of 8.0 wt% has been reported in literature, which is in agreement with the above findings (Murwanashyaka et al., 2001). No discernible impact on water content was found as a result of increased mixing, as seen in Figure 4-7.
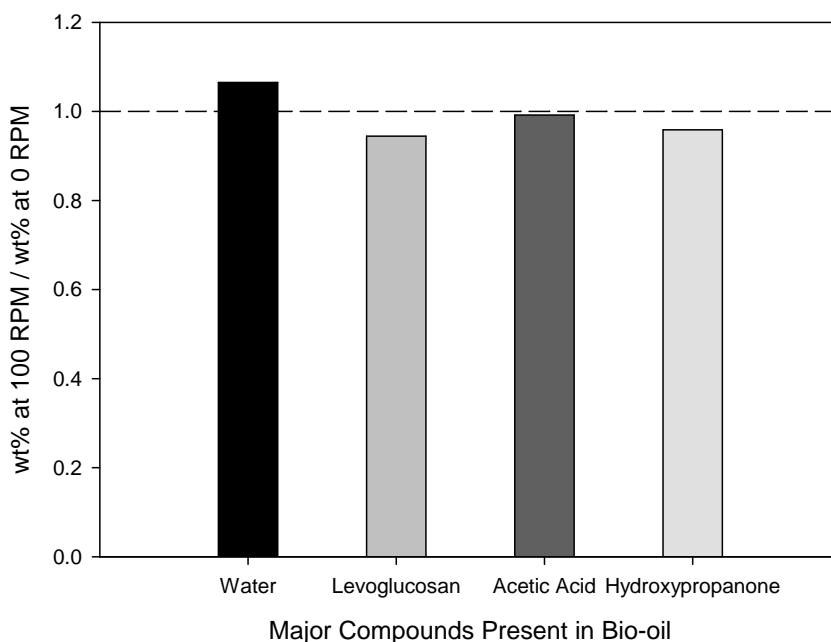
Figure 4-7 - Effect of mixing on bio-oil composition (temperature = 550 °C; particle size = 500-600 μm)

As acetic acid and levoglucosan are among the most abundant compounds present in bio oil, their concentration has been determined using GC-MS/FID analysis. Figure 4-7 indicates the concentrations of water and GC-MS/FID detectable compounds from bio oil obtained at 550°C using 500-600 μm particle sizes. Acetic acid and levoglucosan were found to be the most abundant compounds, respectively. Acetic acid represents 49.7 wt% of the detectable fraction, while levoglucosan encompasses another 8.9 wt%. Hydroxypropanone, and phenolics were also found to be in abundance, and represent roughly 5.6 and 2.3 wt% of the GC-MS/FID detectable fractions. It was found that the composition of these compounds were not impacted by particle-bed mixing in any way, as the ratio of their concentration at 100 RPM compared to 0 RPM was essentially unity. These results indicate that increased mixing within the reactor leads to no drastic changes in the pyrolysis process.

Figure 4-8 - Comparison of GC-MS/FID data for (a) replicate experiments, and (b) varied mixing speeds (temperature =550°C; particle size = 500-600 µm)

Mass spectroscopy data overlays are shown in Figure 4-8(a) and Figure 4-8(b). These overlays demonstrate that the variability among replicate experiments was roughly equal to the variability as different bed mixing levels were used. Multiple overlays conducted using replicate experiments provide confirmation that effective particle mixing was already present within the fluid bed, and applied agitation provided no discernible impact on bio-oil composition.

4.4 Conclusions

It has been determined that, in a non-agglomerating system such as birchwood pyrolysis, the addition of mechanical agitation affords no increase in liquid yields. In addition, it has been found that there was no appreciable impact of applied particle mixing on the composition of the product bio-oil. These results demonstrate that, for effective pyrolysis of non-agglomerating lignocellulosic biomass in a fluid bed reactor, operating parameters such as temperature and particle size require optimization while bed mixing affords limited improvements.

It has also been found that the intermittent solid slug feeder system was fully capable of injecting small particle sizes, with no degradation of feed quality. This indicates that future biomass pyrolysis studies using this feeder technology are capable of optimizing feed particle sizes down to a limit of 150 µm without experiencing injection degradation. It appears that the use of a feeding system which disperses non-agglomerating biomass upon injection, in conjunction with a fluidized bed pyrolyzer, is an effective system upon which particle-bed mixing cannot be improved.

References

Akhtar, J., & Saidina Amin, N. (2012). A Review on Operating Parameters for Optimum Liquid Oil Yield in Biomass Pyrolysis. Renewable and Sustainable Energy Reviews, 16(7), 5101–5109.

Berruti, F. M., Ferrante, L., Berruti, F., & Briens, C. (2009). Optimization of an Intermittent Slug Injection System for Sawdust Biomass Pyrolysis. International Journal of Chemical Reactor Engineering, 7.

Berruti, F. M., Ferrante, L., Briens, C. L., & Berruti, F. (2012). Pyrolysis of Cohesive Meat and Bone Meal in a Bubbling Fluidized Bed with an Intermittent Solid Slug Feeder. Journal of Analytical and Applied Pyrolysis, 94, 153–162.

Bridgwater, A. V, Meier, D., & Radlein, D. (1999). An Overview of Fast Pyrolysis of Biomass. Organic Geochemistry, 30, 1479–1493.

Dai, Q., Jiang, X., Jiang, Y., Jin, Y., Wang, F., Chi, Y., & Yan, J. (2014). Formation of PAHs During the Pyrolysis of Dry Sewage Sludge. Fuel, 130, 92–99.

Davidsson, K. ., & Pettersson, J. B. . (2002). Birch Wood Particle Shrinkage During Rapid Pyrolysis. Fuel, 81(3), 263–270.

Dorez, G., Ferry, L., Sonnier, R., Taguet, A., & López-Cuesta, J.-M. (2014). Effect of Cellulose, Hemicellulose and Lignin Contents on Pyrolysis and Combustion of Natural Fibers. Journal of Analytical and Applied Pyrolysis, 107, 323–331.

Drummond, A. R. F., & Drummond, I. W. (1996). Pyrolysis of Sugar Cane Bagasse in a Wire-Mesh Reactor. Industrial & Engineering Chemistry Research, 35(4), 1263–1268.

Isahak, W. N. R. W., Hisham, M. W. M., Yarmo, M. A., & Yun Hin, T. (2012). A Review on Bio-oil Production from Biomass by Using Pyrolysis Method. Renewable and Sustainable Energy Reviews, 16(8), 5910–5923.

Kim, J. W., Lee, H. W., Lee, I.-G., Jeon, J.-K., Ryu, C., Park, S. H., & Park, Y.-K. (2014). Influence of Reaction Conditions on Bio-oil Production from Pyrolysis of Construction Waste Wood. Renewable Energy, 65, 41–48.

Lira, C. S., Berruti, F. M., Palmisano, P., Berruti, F., Briens, C., & Pécora, A. A. B. (2013). Fast Pyrolysis of Amazon tucumã (Astrocaryum Aculeatum) Seeds in a Bubbling Fluidized Bed Reactor. Journal of Analytical and Applied Pyrolysis, 99, 23–31.

Martínez, J. D., Puy, N., Murillo, R., García, T., Navarro, M. V., & Mastral, A. M. (2013). Waste Tyre Pyrolysis–A Review. Renewable and Sustainable Energy Reviews, 23, 179–213.

Mohan, D., Pittman, C. U., & Steele, P. H. (2006). Pyrolysis of Wood/Biomass for Bio-oil: A Critical Review. Energy & Fuels, 20(3), 848-889.

Murwanashyaka, J. N., Pakdel, H., & Roy, C. (2001). Seperation of Syringol from Birch Wood-Derived Vacuum Pyrolysis Oil. Separation and Purification Technology, 24, 155-165.

Neves, D., Thunman, H., Matos, A., Tarelho, L., & Gómez-Barea, A. (2011). Characterization and Prediction of Biomass Pyrolysis Products. Progress in Energy and Combustion Science, 37(5), 611-630.

Nowakowski, D. J., Bridgwater, A. V., Elliott, D. C., Meier, D., & Wild, P. (2010). Lignin Fast Pyrolysis: Results from an International Collaboration. Journal of Analytical and Applied Pyrolysis, 88(1), 53-72.

Oasmaa, A., & Peacocke, C. (2010). Properties and Fuel Use of Biomass-Derived Fast Pyrolysis Liquids.

Shen, D. K., Gu, S., & Bridgwater, A. V. (2010). The Thermal Performance of the Polysaccharides Extracted from Hardwood: Cellulose and Hemicellulose. Carbohydrate Polymers, 82(1), 39-45.

Gooty, A. (2013). Fractional Condensation of Bio-oil Vapors. The University of Western Ontario.

Uddin, M. N., Daud, W. M. a. W., & Abbas, H. F. (2014). Effects of Pyrolysis Parameters on Hydrogen Formations from Biomass: A Review. RSC Advances, 4(21), 10467-10490.

Yang, H., Yan, R., Chen, H., Lee, D. H., & Zheng, C. (2007). Characteristics of Hemicellulose, Cellulose and Lignin Pyrolysis. Fuel, 86(12), 1781-1788.

cracked to gas, this led to a concentration of refractory, higher viscosity, higher molecular weight compounds in the liquid product.

4. In the non-agglomerating system of birchwood pyrolysis, applied bed mixing had no discernible impact on pyrolysis oil yields. In addition, bed mixing has been found to have no impact on the chemical composition of the product oil. It appears that the use of a feeding system which disperses agglomerating biomass upon injection, in conjunction with a fluidized bed pyrolyzer, is an effective system upon which particle bed mixing cannot be improved.

5.2 Recommendations

In the Fluid Coking Reactor, it was determined that liquid injection at a reduced temperature of 510°C resulted in severe agglomeration and reactor inoperability. Temperature fluctuations of ± 8°C were also observed, leading to increased scatter in the agglomerate distributions for the poorly mixed case. However, the Mechanically Fluidized Reactor had improved temperature control (± 3°C) and experienced higher reproducibility of agglomerate distributions. Quantification of the impact of temperature on agglomeration would provide improved confidence in the solid and liquid yields, leading to a more developed understanding of the impacts of bed mixing and vapor phase cracking. It has been shown that temperature may play a slight role in agglomerate stability, and that industrial Fluid Cokers have been operated at elevated temperatures to avoid defluidization (House et al., 2004; Weber, 2009). There is a need for temperature control improvement on both the MFR and FCR in order to investigate the impact of temperature on agglomerate distributions under consistent operating conditions. This can be accomplished by the following procedure:

1. Improve MFR temperature control by determining the steady-state power requirements of the reactor during continuous injection. The reactor is currently operated using an on-off control which responds to fluctuations, but can be improved upon to provide a more steady power supply. In the proposed mode of operation, instead of setting the desired reactor temperature, the heating power level would be set to achieve a reactor temperature in the desired range. It is likely

the reactor temperature would be much more stable, although it might change slightly during replicate experiments (as heat losses may vary from day to day)

2. Validate the improvements in reactor temperature control by performing MFR coking experiments under short vapor residence time (5 s), poor mixing characteristics (20 RPM) and a temperature of 530 °C. A temperature of 530 °C is suggested to verify the agglomerate distributions under these conditions and determine if temperature control improvement affords further reductions in scatter. Poor mixing characteristics in the MFR are the most representative of agglomerate distributions that are found in the FCR. While short vapor residence time allows for quantification of the liquid and gas yields without significant vapor phase cracking which would interfere with the results.

3. Perform coking experiments under varied reactor temperature to determine the impact of temperature on agglomeration. A range of temperatures from 510 to 550 °C are suggested to determine the limit of reactor operability as well as the temperature that is required to avoid severe agglomeration issues.

In the bitumen-coke systems, it was determined that there were unvaporized liquids trapped in agglomerates in the poorly mixed case. It is recommended that an investigation be undertaken to optimize the bed drying time, in order to determine the total amount of trapped liquid that can be asked and its subsequent impact on yields and liquid quality.

It was determined that the differences in agitator design may have had an impact on agglomerate distributions. This was due to the FCR design requiring a gap between the mixer blade and reactor wall to prevent nozzle damage. It is recommended that the mixer blade be modified on the FCR to scrape the wall while still accommodating the injection nozzle. This will allow for comparable agglomerate distributions between the reactors, allowing for a more in-depth determination of the impacts of vapor phase residence time.

In the non-agglomerating system using birchwood pyrolysis, it was determined that the feeder system and fluidized bed combination were effective at dispersing biomass upon injection, with essentially no improvements to be gained through increased bed mixing. It

would be advantageous to investigate degradation in feed dispersion, similar to the degraded liquid injection studied in the FCR. It is recommended that injection deterioration is studied without the bed mixing system to determine how the fluidized bed responds to poor biomass injection, and the corresponding impacts on the yield and quality of the liquid pyrolysis oil. This would provide information as to whether the inherent mixing within a fluidized bed is capable of compensating for poor initial dispersion of non-agglomerating biomass, and consequently determine if bed mixing has the potential to improve dispersion in a non-agglomerating system or not.

Appendix A – MFR Induction System

The Mechanically Fluidized Reactor and tube reactor have been designed and built with a custom induction heating system. Each system was comprised of an 1800 W induction heater (Hannex, Hong Kong, China). Temperature readings for the reactor were acquired using four type K thermocouples, one NI-9211 thermocouple input (National Instruments, Austin, TX), and one NI-9485 8-channel solid state relay (National Instruments, Austin, TX). A program created in the LabWindows™/CVI platform (National Instruments, Austin, TX) collected the temperature signals and used on-off control to power the induction heaters.

Both the MFR and tube reactor were fabricated from stainless steel. A layer of ceramic fiber insulation was wrapped around the body of the reactors, followed by the induction wiring. The ceramic insulation was used to protect the induction wiring from overheating, as reactor surface temperature overshoots the temperature tolerance of the induction wiring before a steady-state temperature can be attained.

The induction heating system was capable of reaching temperatures of 530 °C in 30 minutes for the MFR, and 120 minutes for the tube reactor. The MFR required a longer heating time due to the thermal inertia of the reactor and bed material (0.400 kg of petroleum coke). Temperature fluctuations in the MFR rarely exceeded ±3 °C, while the tube reactor was maintained within ±5 °C.

Table A-1 - Induction system specifications

<u>Induction Power Supply[1]</u>	
Wattage	1800 W
Frequency	33 kHz
<u>Data Acquisition and Control[2]</u>	
Thermocouple Input Module	NI-9211
Solid State Relay	NI-9485
<u>Induction Wiring</u>	
Wiring specifications	450 °C high temperature braided wire 14 AWG
Total wire length per system	12 m
MFR wiring	24 loops
Tube reactor wiring	38 loops

[1] Hannex, Hong Kong, China

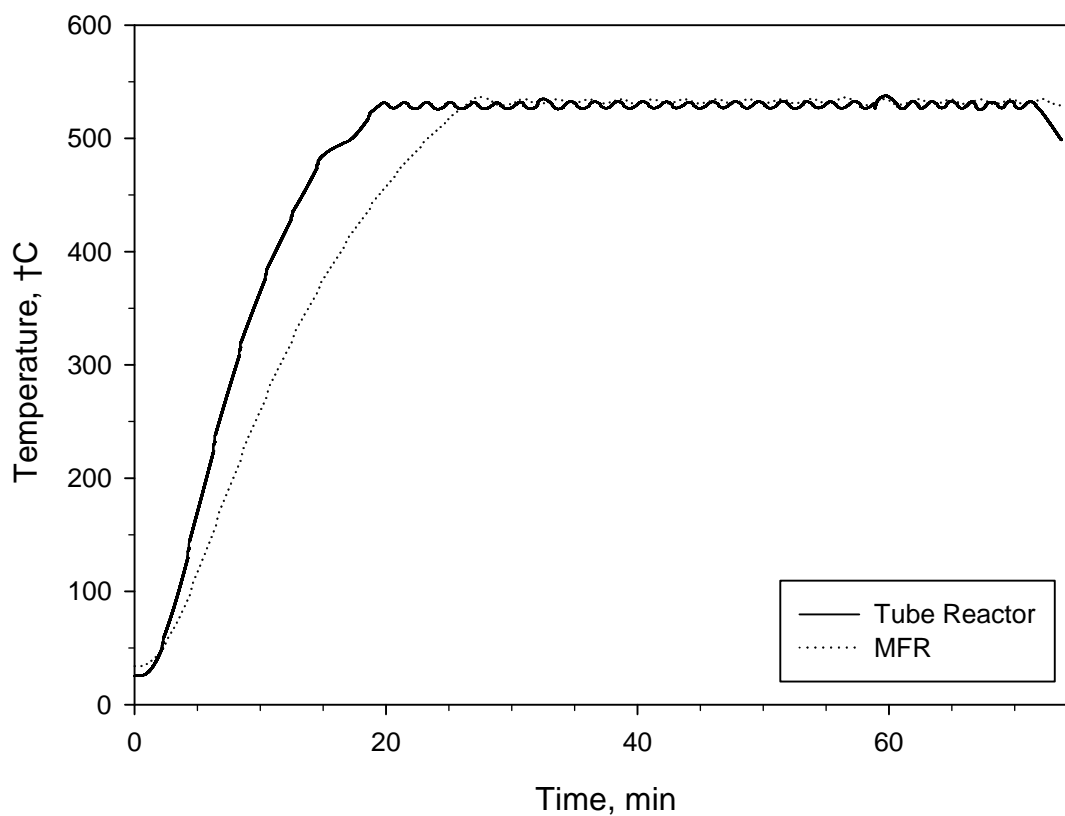[2] National Instruments, Austin, TX

Figure A-1 - MFR system temperature control

Appendix B …Proposed FCR Mixer Design

Figure A-2 - FCR mixer redesign for improved solids mixing

Appendix C …Permission to Reprint Figures

Curriculum Vitae

Name:	Clayton Stanlick
Post-secondary Education and Degrees:	M.E.Sc. Chemical Engineering The University of Western Ontario London, Ontario, Canada 2012-2014 B.E.Sc. Chemical Engineering The University of Western Ontario London, Ontario, Canada 2008-2012
Honours and Awards:	NSERC USRA 2011 Second Prize Winner Capstone Design Competition 2012
Related Work Experience	Graduate Research Assistant The Institute for Chemicals and Fuels from Alternative Resources London, Ontario, Canada 2012-2014 Graduate Teaching Assistant The University of Western Ontario London, Ontario, Canada 2012-2014